TECHNICAL MEMORANDUM

151

Extended range predictions with ECMWF models. I. Interannual variability in operational model integrations

T.N. Palmer, C. Brankovic
and U. Cubasch

Research Department

June 1989

European Centre for Medium-Range Weather Forecasts
Europäisches Zentrum für mittelfristige Wettervorhersage
Centre européen pour les prévisions météorologiques à moyen

ABSTRACT

A set of 30-day integrations made with the operational ECMWF model over a period of three and a half years (from 1985 to 1988) is studied. The impact of model reformulations during this period on the climate drift of the model is assessed, and the level of extended-range forecast skill achieved by the operational model is studied.

Diagnostics of zonal average 30-day mean wind and temperature error show a systematic reduction in the extratropics over three years. It is argued that these improvements are consistent with the changes in model formulation. Eddy fluxes of heat and momentum, and levels of eddy kinetic energy are similarly improved. On the other hand, it is argued that some apparent improvements in the error in tropical divergent flow between 1985 and 1987 may have been associated with interannual variability as the atmosphere evolved toward an El Nino state.

From maps showing the ratio of systematic to total error it is concluded that by the final winter, the middle-latitude extended-range error is almost entirely associated with random errors. This is supported by the growth of the dispersion, or spread, between forecasts initialised 24hrs apart. In particular, for the extended winter 1987/88, it is shown that the asymptotic level of (internal) spread is comparable with the asymptotic level of (external) skill. By contrast, in the tropics, the total error is dominated by the systematic error for all years.

Despite improvements to the model, extended-range forecast skill is modest. Skill has been measured in a spatially filtered three dimensional phase space, spanned by rotated EOF coefficients of 500mb height, which contain the principal weather regimes in the atmopshere. We consider whether in the prediction of 5- and 10-day mean fields beyond day 10 one can obtain as much skill merely by persisting the day 6-10 prediction. For the first winter period, it appears that up to day 16-20, more skill is obtained by carrying on the integration; for the other two winters, it would appear that essentially no more skill is obtained than by persisting the medium range forecast. We demonstrate that in the winter sample of operational model forecasts, skill is correlated with the observed tendency of the first rotated EOF (which can be described as a global version of the Pacific/ North American mode). This indicates that interannual variability in extended-range skill was not primarily associated with any of the model reformulations.

By contrast, the ability to predict monthly mean fields in the tropicsepends primarily on a knowledge of the boundary forcing, including sea surface temperature. It is shown that some aspects of the interannual variability in the summer monsoon circulation can be predicted, in particular the tropical easterly jet anomalies, African rainfall, and, to a much lesser extent, Indian monsoon rainfall. It is hoped these results will provide some encouragement towards the development of fully coupled ocean/atmosphere models for operational seasonal prediction with state-of-the-art numerical weather prediction models as the atmospheric component.

1. INTRODUCTION

This is the first in a series of papers on results from an experimental programme of extended-range integrations of the European Centre for Medium Range Weather Forecasts (ECMWF) numerical weather prediction (NWP) model. The project is part of an international attempt to assess the level of extended-range skill achievable using an operational NWP system (see for example, ECMWF, 1988).

The programme commenced in April 1985, and near the middle of every month the operational ten day integration of the (T106) model was continued out to 30 days, from two consecutive 24hr analyses. This dataset forms the basis of the study in this paper. From a deterministic point of view, these forecasts can be viewed as having been made, at the time of integration, with the most skilful NWP system available at ECMWF. Our principal objectives are to discuss the possible impact of model reformulations during the period of the experimental programme on the aysmptotic climate drift of the operational model, to assess the average level of extended-range forecast skill achieved by the operational model, and to study interannual variability in the skill of extended-range forecast fields both in the tropics and extratropics.

In addition, during the first year of the programme, each T106 integration was repeated at T63, T42 and T21 resolution. This multi-resolution dataset is used in the companion paper by Tibaldi et al (1989), hereafter referred to as II, to assess the influence of horizontal model resolution on climate drift and extended range skill. Finally, approximately every three months, the T63 version of the operational model was integrated for 30 days from nine consecutive 6 hr analyses. The purpose of these was to assess the potential of estimating forecast skill, and to develop techniques for probabilistic forecasting. These T63 forecasts comprised the time-lagged ensembles whose properties are described in Brankovic et al (1989); hereafter referred to as III.

In section 2 we list the forecast initial dates, and describe changes to the operational model over the period of the experimental programme. Indeed, since the first year of extended-range integrations there has been some substantial reformulations of the model, and one would expect these changes to lead to a significant impact on the model climate drift. These are documented in section 3.

It might be expected that a decrease in model systematic bias from one year to the next would be associated with an increase in forecast skill. In order to assess this, we have calculated the extent to which systematic error contributes to the total error, for each 'extended' winter season of October to March. The impact of the model improvements in reducing this ratio in regions of jet maxima can be clearly seen. Throughout much of the

middle latitudes, however, the non-systematic component of error is dominant. This is discussed further in section 4 where we show northern hemisphere skill scores for the three individual extended winter periods. Comparing these scores with the growth of the spread between the individual forecasts initialised one day apart (internal error growth), we assess whether interannual variability in forecast skill is associated with variation in predictability, or with changes in model formulation.

Since the goal of extended-range prediction is to forecast changes in weather regime, we study the skill of predictions of 5-day mean 500mb height projected onto a three dimensional space of rotated empirical orthogonal functions (EOFs). According to Molteni et al (1989), this 3-dimensional space contains six principal local density maxima of atmospheric states, which can be interpreted as weather regimes. Skill scores and phase space trajectories are shown for these truncated fields.

Section 5 of the paper is devoted to a discussion of prediction of monthly mean wind and rainfall in the tropics during the northern summer. As discussed by Charney and Shukla (1981), internal instabilities of the flow on synoptic scales account for most of the interannual variability of monthly mean quantities at mid-latitudes, but cannot explain the observed variability in low latitudes. The latter, they suggested, is due partly to fluctuations in boundary parameters such as sea surface temperature (SST). Since these parameters vary on much larger time scales than the synoptic-scale flow, they should be predictable for longer periods of time. We show that interannual variability in the monthly-mean strength and position of the tropical easterly jet, which appears to be strongly associated with monsoon variability, can be predicted. Also, simulated rainfall anomalies over the African inter-tropical convergence zone (ITCZ) and (to a lesser extent) over India from the four summer seasons do appear to be realistic.

Moreover, it is shown that forecasts of monthly means from integrations initialised one day apart are generally strongly consistent in the tropics. This is contrasted with the predictions of extratropical monthly mean rainfall in the summer extratropics, lending support to Charney and Shukla's hypothesis. Concluding remarks are given in section 6.

2. THE DATABASE AND FORECAST MODEL CHANGES

As mentioned in the introduction, this paper deals with results from extended-range integrations of the operational ECMWF model. The inteations were run twice a month, around the middle of the month, from consecutive 12Z analyses. The initial dates of these integrations are given in Table 1.

For all the integrations, the spectral horizontal resolution of the model remained fixed at T106. However, during the period of the extended-range programme, the model vertical resolution changed, one existing physical parametrization was revised, and one new physical parametrization was introduced. All the model revisions are listed in Table 2.

In May 1986 , the 16-level version of the model was replaced by a 19-level model. This affected the resolution in the stratosphere, and below 200mb there was little change. The principal motivation for the change was to provide better analyses in the stratosphere at standard pressure levels. The impact of this change in vertical resolution has been discussed by Simmons et al (1989). In particular, assessment of a series of 10 day forecasts appears to indicate that the increased vertical resolution had positive impact on the Atlantic jet, the jet split, and associated downstream ridge and trough development in the troposphere. In Simmons (1987), it is shown that the overall strength of midlatitude tropospheric westerlies has been somewhat reduced in the 19-level version of the model.

In July 1986 the parametrization of orographic gravity wave drag (GWD) was introduced, in order to alleviate the tendency toward excessive surface westerly flow in the northern winter. The impact of this scheme on the ECMWF model has been discussed in detail by Miller et al (1989). In addition to a reduction in zonal mean wind, the GWD scheme has a profound impact on the long and synoptic-scale eddy heat and momentum fluxes. Such diagnostics will be shown in the present paper, where we will reference to the appropriate figures in Miller et al (1989).

In September 1986 some changes to the analysis system were made. These changes were primarily of a technical nature, and practically all characteristics of the previous analysis scheme were retained. However, humidity analysis has been changed to the three-dimensional univariate optimal interpolation. It was found that such a new analysis fits observational data better than the previous successive correction method, and makes the analysed fields less moist.

In April 1987 the parametrization of land surface processes was revised (Blondin and Böttger, 1987). These revisions impact principally on surface heat fluxes over the continents, and have larger impact in the summer. Blondin and Böttger found, for example, an overall reduction of about 20% in convective precipitation at the ground. However the revision has little impact on mean wind fields in general, and no significant impact on the tropical easterly jet in particular.

Prior to the introduction of the GWD parametrization, a subgridscale momentum transports in the free atmosphere were represented by a vertical diffusion scheme. However, the

Table 1 Initial dates of operational model integrations used in the present study.

Month	1985	1986	1987	1988
January	--	18, 19	17, 18	16, 17
February	--	15, 16	14, 15	13, 14
March	--	15, 16	14, 15	12, 13
April	15, 16	19, 20	18, 19	16, 17
May	15, 16	17, 18	23, 24	21, 22
June	15, 16	14, 15	13, 14	18, 19
July	16, 17	12, 13	18, 19	16, 17
August	15, 16	16, 17	15, 16	13, 14
September	15, 16	13, 14	12, 13	24, 25
October	15, 16	18, 19	17, 18	--
November	15, 16	15, 16	14, 15	--
December	14, 15	13, 14	12, 13	--

Table 2 Model revisions over period of extended-range forecast programme.

Date	Modification
13 May 1986	19-level model
15 July 1986	GWD parametrization scheme
9 September 1986	New analysis
7 April 1987	Revised surface and subsurface parametrization
5 January 1988	Revised vertical diffusion scheme

values of diffusion coefficients used prior to January 1988 caused free atmosphere dissipation and associated vertical smoothing of jets to be excessive. A revised scheme was introduced in January 1988 in which the vertical diffusion term no longer operated above a diagnosed boundary layer top, except when static instability is generated (Miller 1988). Tests indicated that this revision substantially reduced errors in the level of eddy kinetic energy.

Since the change to the vertical diffusion parametrization was made during the extended winter period, (October to March; hereafter OM) we re-ran the three pairs of forecasts from October, November and December 1987, with the revised vertical diffusion scheme (though we did not re-assimilate the initial data). The results presented below will therefore be such that within each of the three OM periods, there have been no changes to the forecast model.

3. INTERANNUAL VARIABILITY IN SYSTEMATIC ERROR

3.1 Zonal average diagnostics

A number of zonal mean diagnostics of heat and momentum are shown below for the three OM T106 forecasts. Similar diagnostics are given in the companion paper II on the impact of horizontal resolution on systematic error.

Fig 1, left, shows the 30-day average OM systematic error in zonal mean zonal wind. For winter 1985/86 (Fig 1a) we find excessive westerlies in the extratropics, particularly in the northern hemisphere (NH), extending from the ground to the top of the model. In the northern tropical troposphere, there are substantial easterly errors, becoming westerly in the tropical stratosphere.

In the second winter (Fig 1b), the tropical errors are largely unchanged, but there is significant reduction in extratropical westerly errors, particularly in the NH stratosphere and upper troposphere. This is clearly consistent with the model changes introduced between these two winter seasons (see Table 2). In particular, the impact of GWD would certainly be in the sense observed between Figs 1a,b (compare, for example, with Figs 1c and 22 of Miller et al, 1989). (This has been confirmed by Brankovic (1989) who compared OM 1986/87 extended-range integrations of the ECMWF T63 model which included 19 levels but no GWD, with T63 integrations which included both 19 levels and GWD. In the 'no GWD' runs, the mean NH lower stratosphere westerly wind error exceeds 8 m/s at about 45N, having almost identical structure as shown in Fig 1a. This would confirm that the reduction in westerly bias between 1985/86 and 1986/87, see Fig 1, comes primarily from the GWD parametrization.)

In the third winter (Fig 1c), there is some further reduction in NH extratropical westerly error, though the tropical easterly error appears to have increased in the upper troposphere.

It could be argued that the apparent reduction in systematic error over the three winters merely reflects interannual variability in the real atmospheric circulation. For example, if the extratropical zonal mean flow in the second winter was significantly stronger than the first winter, the model may show a reduction in systematic error in the absence of any change in model formulation. Fig 1d-f show the verifying analysis anomalies relative to the three-year mean. (Note the reduced contour interval relative to Fig 1a-c.) It is clear that, in general, the reduction in systematic error is genuine, except perhaps in the equatorial stratosphere, where the analysis shows strong westerly anomalies for the third year, presumably associated with the quasi-bienniel oscillation.

It is interesting to examine the evolution of these systematic errors as a function of forecast time, in order to assess the extent to which the climate drift of the model can be deduced purely from systematic errors within the medium-range period. Fig 2 shows the zonal mean zonal wind error averaged from 300-30mb for the three OM periods. The errors are growing strongly at the end of the medium range (denoted here by the vertical lines drawn at day 10). Moreover, the evolution of systematic error in the first 10 days can give a misleading impression of the overall longer term climate drift. For example, the reduction in the 30-day mean NH extratropical zonal mean wind error between the first, second and third winter (Fig 1a,b,c) is not apparent in the first 10 days of integration. Indeed, in the first 10-days during the third winter, a 4m/s error is evident by about day 5, earlier in the forecast period than in the previous two winters. However, these errors barely exceed 4m/s throughout the 30 day period, whilst in the second winter they exceed 6m/s by about day 18, and in the first winter they exceed 8m/s by about day 16 reaching 10m/s towards the end of the forecast period. As commented above, 30-day mean tropical easterly errors appear to have increased in the third winter; this is quite clear from Fig 2, where, for the third winter, there are values in excess of 8m/s in the last 5 days of integration. Indeed it is unclear from this figure whether the climate drift of the model has asymptoted at day 30. We believe these remarks highlight the importance of extended-range integrations in the assessment of possible model reformulations, even within a purely medium-range NWP environment.

For reasons of space we shall not show diagrams of mean temperature error. However, the NH high latitude stratospheric cooling in the first extended winter is reduced in the second extended winter, and has become a little too warm by the third winter. The overall warming in the tropics persists throughout the period.

Fig 3 shows errors in momentum flux, decomposed into zonal wavenumbers 1-3 (left) and wavenumbers 4-9 (right). In II, it is argued that the excessive long-wave poleward momentum fluxes in the stratosphere centred at about 45N are the result of spurious reflection of Rossby-wave activity from the top of the model. Consistent with this speculation, one would expect a decrease in this error with the increase in vertical resolution, and the introduction of GWD. Such a decrease is indeed observed between the first and second winters. It is also argued in II that the insufficient long-wave equatorward momentum flux in high latitudes, and the excessive synoptic-scale momentum flux in lower latitudes, simulated during the first winter (see Fig 3 a,b), are the consequence of inadequate orographic forcing in the ECMWF model. A clear decrease in the synoptic-scale momentum flux errors can be seen between the first and second winters, after the introduction of orographic GWD. A decrease in high latitude poleward momentum flux error is also observed, though at the same time there appears to be an increase in error in middle latitudes. The maximum error in the third winter is positioned close to the latitude of maximum momentum-flux gradient in the analysis, and therefore corresponds to an error in the latitudinal positioning of maximum gradient. This latter error was not anticipated on the basis of experiments with the GWD parametrization alone (see Miller et al, 1989, Fig 18).

As shown in Fig 4, the underestimation in stratospheric poleward heat fluxes is substantially reduced between the first and second winters, consistent with expectations on the basis of GWD experiments (see Fig 18 of Miller et al, 1989). On the other hand, near the tropopause, there is an increase in (synoptic wave) heat flux error in the NH in the second winter, but this is reduced in the third winter consistent with the effective removal of free-atmosphere vertical diffusion.

One of the principal improvements to the model climate drift in the third winter is the reduction in the error in eddy kinetic energy. This is shown in Fig 5. In the second winter, it appears that the introduction of 19 levels and GWD had some impact in the stratosphere, but little in the troposphere. For the third winter, reduction of the error in eddy kinetic energy throughout the troposphere is self evident.

3.2 Geographical distribution of extratropical systematic error and its contribution to total error

Fig 6 shows the average 30-day mean 500mb height error maps for forecasts in the NH and SH for the three OM seasons. It can be seen that the negative height errors over the northeast Pacific and northeast Atlantic are reduced in the second winter, particularly over the Atlantic (cf Fig 6 a,c). There is, however, an increase in geopotential height error over the central Pacific between the first and second winter. (This may be associated with

atmospheric interannual variability; the 1986/87 El Nino event was at its peak during this winter period.) During the third winter period (Fig 6e) there is an overall reduction in height error; the only significant errors are over the Pacific and east Asian seaboard, though smaller in comparison with the two previous winters. Whilst the error pattern over the northern Pacific and northern Atlantic shown in Fig 6a is typical of the 'zonalisation' in earlier versions of the ECMWF model (see for example, Wallace et al, 1983), from 1986 this error has not only been reduced, but its pattern is also changed.

In the SH for the first year (Fig 6b), there is a band of positive height error in midlatitudes exceeding 4 dam. There is a small region at about 60S near the date line where negative height errors exceed 5dam. The character of these errors has been changed little in the second year (Fig 6d). The largest change comes in the third year (Fig 6f), when, except for some rather isolated regions, errors are everywhere less than 4 dam.

Another way of assessing the impact of model reformulations on model skill is shown in Figs 7 and 8. These figures show for each winter period, the fraction of total daily mean square error in 500 mb height contributed by the systematic error. This fraction is computed for days 21-30 of each forecast; over this time daily forecast errors are, to a good approximation, statistically stationary. The ratio shown in Figs 7 and 8 can be written as

$$\left[\frac{1}{120}\sum_{j=1}^{12}\sum_{i=21}^{30} E_{ij}(x,y)\right]^2 \Big/ \frac{1}{120}\sum_{j=1}^{12}\sum_{i=21}^{30} E_{ij}^2(x,y)$$

where $E_{ij}(x,y)$ is 500mb height error. The index i runs over forecast day (ie from 21-30), and the index j runs over forecast cases (ie from 1 to 12 for the set of OM forecasts).

For the first NH winter period (Fig 7a), it can be seen that the contribution of the systematic error to the total error is considerable, particularly in the jet regions (see also Hollingsworth et al., 1987). Over the east Asian seaboard the systematic error contributes up to 70% of the total daily mean square error (over 80% in terms of the ratio of RMS errors). Across the Eurasian land mass, values exceed 30% everywhere in jet regions. In high latitudes values are generally smaller, though they reach almost 60% over the Bering strait.

These values are generally reduced in the second NH winter,Fig 7b, (except over the subtropical central north Pacific, where as shown above, 30-day mean systematic error increased. On the other hand, the character of the error ratio remains the same as in the first winter. There is a considerable overall reduction, however, in the third winter (Fig

7e) with the only significant area of high ratio in the extratropics lying over the east Asian seaboard and the subtropical east Pacific. Clearly this major reduction is attributed to the impact of the reduction in free-atmosphere vertical diffusion.

A similar reduction in the relative impact of the model systematic error on total daily mean square error, can be seen in the southern hemisphere (Fig 7 b,d,f), with the only significant area of high ratio in the extratropics in 1987/88 lying over Australia.

In the tropics, on the other hand, systematic error is a substantial fraction of total error over much of the area during all three winters (see Fig 8). There is no apparent reduction in the ratio over the three years. For all years, there are maxima over the eastern Pacific/central American region, and over or near Africa. For 1986/87 and 1987/88, the 60% contour (almost 80% in terms of RMS) covers most of the tropics. It should be noted, however, that the model changes introduced over the period of three years were aimed mainly to reduce model systematic deficiencies in mid-latitudes.

3.3 Geographical distribution of systematic error in tropical divergent flow

In Fig 9 (left) is shown the 30-day mean 200mb velocity potential error for T106 forecasts between April and September. As discussed in II, the sense of the error in the first year is such as to give insufficient divergence over Indonesia, and insufficient subsidence over Africa and the south Atlantic.

From Fig 9, it appears that the systematic error decreases to relatively small levels between 1985, and 1987, and then increases somehat in 1988. However, as discussed above, before concluding that this reduction represents the effect of changes in model formulation, it is first necessary to discount possible influences of atmospheric interannual variability.

In the right hand column of Fig 9 is shown the analysed 200mb velocity potential for the same four extended summer periods. It can be seen that there is apparently substantial interannual variability in the magnitude of the Indonesian minimum decreasing between 1985 and 1986, and again between 1986 and 1987, and increasing again in 1988 (ie in the same sense as the model systematic error). This is consistent with interannual variability in the El Nino/ Southern Oscillation (ENSO) phenomenon, leading to a significant warm phase in 1987 (see, for example, The climate system monitoring monthly bulletins of the World Meteorological Organisation). During the warm phase of ENSO, sea surface temperatures in the east Pacific are higher than average, and the Walker circulation is weakened, leading to the anomalies in divergent flow over the Pacific as shown in Fig 9. Late in 1987, the ENSO cycle reversed, the Walker circulation intensified, and consistent with this, the analysed divergent flow in Fig 9 shows increased gradient over the Pacific in 1988 relative to 1987.

Similar conclusions can be reached for the nondivergent circulation errors. For reasons of space these will not be shown. However, consistent with the above discussion, we have found that upper tropospheric tropical easterly errors were smaller during 1988 than 1987. (During an El Nino year, analysed tropical easterlies tend to be weakened; eg Palmer and Mansfield, 1986).

Hence it would appear that one cannot dismiss the role of interannual variability in explaining the apparent change in systematic error in the tropical flow. Indeed, on the basis of these results, and those shown in Fig 8, it would appear that the changes in model formulation since the beginning of the extended-range forecast programme have not fundamentally improved the basic character of the tropical systematic errors. However, as shown by Tiedtke et al. (1988), the 1985 movel change already represented a big improvement over the previous model.

4. EVOLUTION OF MODEL SKILL OVER THREE EXTENDED WINTERS

4.1 Interannual variability in extended-range skill

In earlier sections we have discussed the apparent improvement in systematic error since the beginning of the extended-range forecast programme. In this subsection, we pose the question; have these model improvements led to any change in extended-range skill?

In Fig 10a we show the conventional NH anomaly correlation coefficient (ACC) of 500mb height, averaged over the 12 forecasts for each season, for 10-day and monthly mean fields, for each of the three winters. It can be seen that, despite the improvements to the model climate drift, there is no clear monotonic improvement in skill over the three years. Indeed, over the 30-day period, one cannot clearly distinguish between the first and third winters in terms of ACC.

Fig 10b shows the intrinsic error growth over the three OM periods in terms of the ACC of 500mb height within each of the twin forecasts. It is interesting to note that growth and apparent asymptotic level of spread in the third winter is noticeably larger than the values in the first two winters. This is also observed in terms of RMS spread (not shown), which for the third winter asymptotes close to the level of persistence at days 16-25. This, in turn, gives the upper limit for potential predictive skill for 10-day mean fields.

It would therefore appear from Fig 10 that the recent improvements in model formulation have not had a strong impact on time-mean forecast skill throughout the 30-day range. This may indicate that the impact of intrinsic atmospheric interannual variability was dominant (see also below). Consistent with results above, the reduction in free atmosphere vertical diffusion appears to have led to more realistic internal error growth statistics.

4.2 Forecast skill of large-scale weather regime transition

We now address a crucial question in the assessment of the extended-range programme: is there any indication in results over the last three winter periods, of skill in the prediction of weather regime transitions beyond the medium range?

In a recent paper (Molteni et al, 1989), regimes of the northern extratropical circulation in winter were identified as local density maxima, or clusters, of atmospheric states in a 5 dimensional phase space generated by the leading EOFs of 500mb eddy (i.e. deviation from zonal mean) geopotential height fields. Six principal clusters were found. Further analysis revealed that a 3 dimensional subspace contained these six clusters. The three rotated EOFs of 500mb height which define orthogonal axes for this subspace are shown in Fig 11. Whilst the clusters, and not the rotated EOFs, represent the actual circulation regimes, it is worth commenting on the patterns associated with these EOFs. Rotated EOF 1 is very similar in structure to the Pacific/North American pattern identified by Wallace and Gutzler (1981), except that the wave pattern over the Atlantic and Eurasia has now a more substantial amplitude. Rotated EOF 2 has a clear wavenumber 3 pattern, with ridges in areas of strong low-frequency and blocking variability (see for example Dole, 1986). Rotated EOF 3 has strong amplitude in the Euro/Atlantic sector where it resembles the Eurasian teleconnection pattern described by Wallace and Gutzler (1981).

Since the principal weather regimes of the northern winter lie in the space spanned by these three rotated EOFs, and since the principal objective of extended-range forecasting is the prediction of weather regime (rather than instantaneous weather), we study in detail the verification of the wintertime extended range forecasts (November to February inclusive) by projecting each forecast and verifying 500mb height field onto these three rotated EOFs.

Results of ACC and tendency correlation coefficient (TCC) skill scores of 5-day mean height fields, projected onto these three EOFs are summarised in Table 3 a, b. The TCC is the correlation of observed and predicted differences between a given 5-day mean, and the 5-day mean immediately preceding it. Table 3a shows the average ACC (over all forecasts in each winter) for the three individual winters (1985/86, 1986/87, and 1987/88). In the first five days, the height pattern is predicted with ACC > 0.9 for all winters. For days 6-10, there is already considerable interannual variability, with the first winter being the most skilful, the second winter being the least skilful. In this sense, these filtered ACC scores are consistent with the conventional ACC estimates of skill for the first ten day mean, shown in Fig 10. Beyond day 10 the ACC for winter 1 remains positive throughout the forecast period. For winters 2 and 3, on the other hand, the ACC for days 16-20 are negative. For days 21-30, there is an apparent 'return of skill' during the second and

a

ACC Winter	1 - 5	6 - 10	11 - 15	16 - 20	21 - 25	26 - 30
85/86	0.91	0.82	0.26	0.04	0.05	0.08
86/87	0.94	0.32	0.48	- 0.15	0.17	- 0.04
87/88	0.97	0.61	0.33	- 0.22	0.29	- 0.10

b

TCC Winter	(1-5) -> (6-10)	(6-10) -> (11-15)	(11-15) -> (16-20)	(16-20) -> (21-25)	(21-25) -> (26-30)
85/86	0.74	0.23	0.30	- 0.33	0.03
86/87	0.73	- 0.32	- 0.17	0.37	- 0.21
87/88	0.70	- 0.15	0.15	0.08	- 0.04

c

ACC Winter	1 - 10	11 - 20	21 - 30
85/86	0.90	0.32	0.14
86/87	0.44	0.05	0.05
87/88	0.81	- 0.05	- 0.12

d

TCC Winter	(1-10) -> (11-20)	(11-20) -> (21-30)
85/86	0.47	0.20
86/87	0.06	0.16
87/88	- 0.19	0.01

Table 3

a) 5-day mean anomaly correlation efficient for 500mb height fields projected onto the rotated EOFs shown in Fig 10; b) 5-day mean tendency correlation coefficient for 500mb height fields projected onto the rotated EOFs; c) 10-day mean anomaly correlation coefficient for 500mb height fields projected onto the rotated EOFs shown in Fig 10; d) 10-day mean tendency correlation coefficient for 500mb height fields projected onto the rotated EOFs.

third year, though it is difficult to attach any particular significance to this. Differences between Table 3 and Fig. 10 result from different sampling (only November to February in Table 3), and because data in Table 3 were derived from filtered eddy fields only.

Table 3b shows TCC values. The numbers in the first column indicate that the predicted transition between days 1-5 and days 6-10 is correlated with the observed transition with a coefficient of at least 0.7 for each of the three years. The correlation between the predicted and observed transition between days 6-10 and 11-15 is positive for the first year, and comparable with the ACC shown in table 3a. For the second and third years, however, the TCC is negative. This indicates that for the last two years, a more accurate forecast of days 11-15 could be obtained by persisting the day 6-10 prediction for which the TCC = 0 (see also Saha and van den Dool, 1988).

The ACC and TCC skill scores of 10-day mean height fields are summarised in Table 3 c,d respectively. As above, it can be seen that forecasts are most skilful for the first winter, where ACC > 0 for all three 10-day means. Note also, for this winter that TCC > 0 for the tendency between days 1-10 to 11-20, and between days 11-20 to 21-30 (Table 3d). For the second winter TCC beyond days 1-10 is only just positive, and for the third winter, persisting the forecast of the first 10-day mean would, on average, be more skilful than continuing the integration. Taking the three winters togather, it would appear that skill is lost between days 10 and 20, though over a significant fraction of forecasts, skill is maintained to the end of this period.

In order to give a visual impression of the overall level of skill of forecasts of the large-scale flow up to day 15, we show in Fig 12 trajectories of the winter integrations and verifying analyses for the three years, in the space spanned by the first two rotated EOFs. (For reasons of space we do not show trajectories projected onto the third EOF, though the general conclusions made here are valid for the trajectories in the third dimension.)

Each trajectory in Fig 12 consists of three line segments. The line segments join values for the mean of days 1-5, 6-10 and 11-15. The two forecast trajectories have closed arrowheads labelled "1" and "2" and the verifying analysis trajectory has an open arrowhead labelled "0". The arrowheads lie on values for days 11-15. The left hand column shows forecasts from November 15 to February 1986, the middle column from November 1986 to February 1987, and the right hand column from November 1987 to February 1988.

It is clear from Fig 12 that predictability is, on average, marginal at days 11-15. Nevertheless, there are clearly some cases when both of the twin forecasts were skilful at

this range (eg the 'close to perfect' predictions for February 1986; this case is discussed in more detail in III). There are others (eg January 1988) where one of the twin forecasts evolved correctly, whilst the other was utterly eroneous. There are cases (eg November 1985) where both forecasts, although marginal, give an approximately correct sense of direction of the phase-space evolution of the observed flow. Finally, there are cases (eg December 1986) when both integrations, although consistent in their prediction of flow evolution beyond day 10, are both incorrect.

The visual impression of these phase space trajectories confirm the results of the objective skill scores. However, it is important to judge the viability of extended-range forecasting not only in terms of the mean level of skill, but also by the ability to identify a priori, those forecasts with above average levels of skill. This topic is discussed in detail in III which addresses techniques of time-lagged ensemble forecasting.

We conclude this section by discussing the possible relationship between forecast skill and transitions between particular weather regimes. As discussed in Palmer (1988), there appears to be a clear dependence of extended range predictive skill on the sign of the PNA index of either the observed or predicted flow. This relationship has been studied in more detail by Molteni and Tibaldi (1989) in terms of the rotated EOFs used in this section. In particular, Molteni and Tibaldi found that forecast skill scores in the medium range had a clear bimodal distribution when the rotated EOF1 had negative coefficient. They related this to the existence of two major atmospheric clusters found by Molteni et al (1989), in the region of phase space where the rotated EOF1 coefficient was negative. In Fig.13 we show scatter diagrams of the TC skill score between days 1-10 and 11-20, and the tendency of the verifying rotated EOF 1 coefficient between days 1-10 and 11-20. There is a correlation of 42% between these two sets of data, with the most skilful forecasts being associated with transitions to positive EOF1 coefficient. Since positive EOF1 has positive PNA index, the results from this study are consistent with those of Palmer (1988). Note that forecasts with the highest tendency of rotated EOF1 come from the first year (triangles), when extended-range forecast skill was highest. For EOF2 and EOF3, the correlation is much smaller. These results again indicate that interannual variability in extended-range skill was not primarily associated with any of the model reformulations.

5. PREDICTION OF TROPICAL MONTHLY MEAN WIND AND RAINFALL

As discussed in the introduction, internal instabilities in the extratropical wintertime flow appear to be able to account for much of its observed variability up to timescales of a month (eg, Palmer, 1987). Hence the variation of boundary forcing on the extratropical flow is not a dominant source of observed extratropical wintertime low-frequency variability. As a result, monthly timescale prediction in the extratropical wintertime appears to be principally an initial value problem.

On the other hand, as suggested by Charney and Shukla (1981) and demonstrated in a series of GCM experiments by Manabe and Hahn (1981) and Lau (1981), the internal dynamics of the tropical atmosphere can only explain a fraction of monthly timescale interannual variability of the atmospheric flow. Indeed in our discussion in section 3, we noted that aspects of the model tropical systematic error were correlated with anomalies in the boundary forcing. In this sense, it would appear that an important component of the tropical atmospheric prediction problem on timescales of a month or more is associated with an ability to predict this boundary forcing.

In common with most GCMs, some of the land surface processes in the ECMWF model (eg associated with variability in surface temperature, soil moisture) are interactive. However, over the ocean, surface temperatures throughout the integration are held constant at their initial values. Such noninteractive ocean boundary conditions may be sufficient for monthly prediction, but are probably insufficient for seasonal timescales. Whilst seasonal prediction with coupled ocean atmosphere models represents a major goal of the World Climate Research Programme, it is important to ascertain first that accurate monthly prediction in the tropics with a high resolution NWP model is feasible with only partially interactive boundary conditions. A successful outcome may provide some stimulus for the development of operational NWP models with fully interactive boundary forcing. Moreover, as suggested by Shukla et al (1988), monthly mean fields during severe drought or flood monsoon years are often broadly representative of the season as a whole.

It can also be mentioned that an ability to simulate accurately tropical low-frequency variability has a profound influence on extratropical extended-range forecast skill. This has been shown in a companion paper (Ferranti et al, 1989) in which a number of extended range integrations were rerun with tropical winds and temperatures relaxed towards the verifying analysis. The results of Ferranti et al, therefore provide additional motivation for the analysis in this section.

In sections 5.1 and 5.2 we study the prediction of interannual variability in wind fields over the African/Asian monsoon region during the summer periods from 1985 to 1988, and focus on India and the Sahel to study the regional prediction of monthly mean rainfall. Motivated by these results, we discuss briefly in section 5.3 predictions of monthly mean rainfall over Europe and North America for the same period.

5.1 Summer monsoon wind

Fig 14 shows the verifying analysis of 30-day mean 200mb winds over the eastern tropical hemisphere, for the four individual mid June to mid July periods from 1985 to 1988. Diagnostic studies (Newell and Kidson, 1984 and Lu and Ding, 1989, for example), have

suggested a strong association betwe the strength of the tropical easterly jet and the intensity of seasonal monsoon rains over both Africa and India.

Interannual variability in the strength and position of the tropical easterly jet is apparent. Values greater than 20m/s are shown stippled. During 1985 (Fig 14a), the analysed 20m/s isotach extended from Indonesia to east Africa, with the 10m/s isotach extending across most of the eastern hemisphere. During 1986 (Fig 14b), the extent of the 20m/s isotach is clearly reduced, and over western Africa, the 10m/s line is broken. The analysis for 1987 (Fig 14c) shows a further weakening of the tropical easterly jet. The 20m/s isotach is barely evident, and the 10m/s contour over Africa is well broken. During the 1988 period (Fig 14d), the strength of the easterly jet increased significantly compared with 1987 values. It is worth noting that the position of the jet core in 1988 is shifted further west than any of the earlier years, and over Africa is the strongest of the four year period. Interannual variability in the tropical easterly jet for other summer months is qualitatively consistent with these results (not shown).

Fig 15 shows the forecast monthly-mean 200mb winds for the four years. For each year, we show results from only the first forecast from the consecutive initial conditions. However, as will be shown below, tropical predictions from the twin forecasts are very similar. During 1985, the forecast 20m/s isotach extended from about 90E to 15E. During the 1986 period, the stippled region where winds exceed 20m/s is reduced, extending now from the tip of India to central Africa. For 1987 it can be seen that there is only a very small region of 20m/s winds over east Africa. In 1988, the forecast easterly winds increased in intensity, extending in both cases as far east and west as they did in 1985. It is worth noting that the stippled region in both forecasts for 1988 extended north of 15N over east Africa and the Arabian sea. The forecast 20m/s winds failed to reach this far north in any preceding year.

A number of points can be made comparing Figs 14 and 15. Firstly, it is clear that there is a systematic bias in the geographical position of strongest winds in the forecast fields. The forecast 20m/s isopleth is clearly shifted west compared with the analysed values. (As shown in II, there is also a bias in the 850mb monsoon flow, with the low-level jet off the Somali peninsula and the curvature of the flow towards India being underestimated.) However, despite this systematic bias, the interannual variability in the forecast 200mb winds have clearly been correctly predicted at least qualitatively, with a monotonic decrease in strength between 1985 and 1987, and an increase in 1988.

Although not shown here, we have studied 30-day mean forecast winds from other summer months, and, in addition, the 10-day mean winds comprising the monthly mean. In general forecast winds from later months in the season are not as skilful as those shown in Fig 15.

Moreover, for all months, the systematic errors have grown to a sufficiently large amplitude by days 21-30, that little predictive skill is left. In this sense, the skill of the monthly mean fields is dominated by skill in the first 20 days.

5.2 Summer monsoon rainfall

In this section, we show some regional maps over Africa and India of monthly mean predicted rainfall. In order to attempt to verify these rainfall amounts, we have taken, from the operational ECMWF forecast archive, accumulated 24hr rainfall amounts averaged over thirty Day-1 operational forecasts, within the period of the extended-range forecast, and used that as 'truth'. According to Datta and Hatwar (1988) this 24hr accumulated rainfall gives a reasonable approximation of monthly-mean monsoon rainfall over India, and values compare well with Jaeger's climatology (1976).

In Fig 16 and 17 (top panels) we first show the monthly-mean predicted rain for mid June to mid July and for mid July to mid August, averaged over the four years. This is compared with the 'verifying' rain over exactly the same period (Figs 16 and 17; bottom panels). Over Africa, it can be seen that the major maxima over the west coast and the Ethiopian highlands are well simulated. The northward displacement of the ITCZ between the two monthly periods is correctly captured.

Over India, rainfall is reasonably well simulated though, consistent with systematic errors in low-level wind, the rainfall maximum over the west coast is positioned somewhat too far north. The interior of northern India is also too wet especially in the July forecasts, though the rain shadow effect to the east of the western Ghats is well simulated. The maximum over the Bay of Bengal is well simulated. The apparent weakening of 30-day mean forecast rainfall amount over much of the Indian ocean may be associated with problems related to the initial 'spin-up' of the model during the first few days of the forecast period, giving erroneously strong verifying rain.

Figs 18 and 19 show the monthly-mean 'verifying' rainfall anomalies (deviations from the 24-hr accumulated mean) over Africa and India for mid June to mid July, and mid July to mid August (respectively). The corresponding 30-day mean predictions (deviations from the 4 year average 30-day mean field) are shown in Fig 20 and 21.

As suggested above, it appears that African rainfall anomalies are generally correlated with the strength of the tropical easterly jet. During 1985, the 'verifying' rainfall showed positive values in the ITCZ over Africa during both 30-day periods. During 1986, as the jet weakened across western Africa (Fig 14b), rainfall anomalies became negative in the west, but remained positive in the east. Again note the consistency between the two months. 1987 was a drought year across the Sahel, where rainfall anomalies were negative

across most of the region. In 1988 anomalies were positive in the west and in the extreme east, where the excess rainfall in the Ethiopian highlands was associated with the well-publicised flooding in Sudan.

The 30-day mean forecast rainfall anomalies from both integrations (Figs 20 and 21) show anomaly fields which accord reasonably well with the 'verifying' rain over Africa. Note the consistency between forecasts initialised 24hrs apart, an indication of the relative unimportance of internal instabilities for these monthly tropical predictions. In 1985, both forecasts from each of the two monthly periods show a ba of positive rainfall anomaly extending from the west coast across to about 40E. These positive anomalies extend further north for the second 30-day period. During 1986, particularly for the July forecasts, anomalies generally showed negative values on the west coast and over the Gulf of Guinea, and generally positive values over east Africa. During 1987, all integrations correctly predicted negative rainfall anomalies over much of the ITCZ from the west coast to the east. For 1988, the integrations show a partial (though probably insufficient) return to more normal conditions. Note in particular, however, the positive forecast rainfall anomalies over the eastern Ethiopian highlands, particularly for the July forecasts.

Over India, the 'verifying' rainfall (Figs 18-19) show positive anomalies (for both months) over the west coast in 1985. 1987 was a drought year, as suggested by the extensive regions of negative anomalies. 1988 saw a return to more normal monsoon rainfall, though note the positive anomalies over the Himalayan foothills, presumably associated with the severe flooding of Bangladesh.

It can be seen that the predictions of Indian monsoon rainfall anomalies (Fig 20-21) are not as accurate as for the African monsoon. Nevertheless, some of the more important features do appear to have been forecast for the first 30-day period (June-July). For example, during the drought year, 1987, there are indications of negative anomalies, at least to the north. During 1988, the strong positive anomalies over the Himalayan foothills also appear to have been correctly predicted. For the second 30-day period (July-August), on the other hand, the forecasts appear to be much poorer. For example, the 1987 drought is barely captured. (This is consistent with our comment earlier that the prediction of the tropical easterly jet was poorer for the July forecasts than for the June forecasts.) It is likely that the relative poorness of the Indian monsoon predictions is associated with the fact that the climate drift of the model is more severe over the Indian ocean than over Africa. In addition, low-frequency variability associated with, for example, the 30-60 day oscillation is not well predicted with the ECMWF model. Such variability could play an important role in monthly-timescale prediction of the large-scale flow over the Indian Ocean; less so over Africa where the amplitude of the oscillation is much weaker.

In conclusion, it would appear that some aspects of the large-scale tropical monsoon circulation, and even more regional rainfall anomalies have been predicted on a monthly timescale, particularly for the African region. This supports the results of Folland et al (1986) and Owen and Folland (1988) that interannual and interdecadal variability in world wide SST is responsible for drought over Africa, and that seasonal forecasts of African rainfall based on a knowledge of worldwide SST can be made. Indeed since the observed anomalies are fairly persistent from one month to the next, the 30-day anomalies can be treated approximately as proxies for seasonal timescale rainfall and wind anomalies. In this paper we shall not pursue further the question of the role that the boundary forcing (land processes and ocean temperatures) had in these forecasts: this will be the subject of a further investigation (see, for example, Palmer and Brankovic, 1989). However, these results suggest that with a fully interactive atmosphere/ocean/land model, seasonal timescale forecasting of monsoon rainfall could become a practical reality. On the other hand, it must be emphasised that before this can be achieved (at least using the ECMWF model), substantial reduction in tropical systematic error is necessary.

5.3 Summer extratropical rainfall

It is of interest, for comparison with the tropical results above, to discuss briefly some summer monthly-mean rainfall predictions in the extratropics, over Europe in particular. Compared with the winter, internal instabilities in the northern summer extratropics are weak, and the impact of anomalous boundary forecing may be comparatively large. We. concentrate on the period mid June-mid July below.

Rainfall anomalies over Europe are shown in Figs 22 and 23 in the same form as in Figs 18 and 20 for the monsoon area. For 1985, the verifying rainfall shows a coherent pattern with positive anomalies over much of Europe. Over northern Europe, the forecast patterns appear skilful, though elsewhere, the two forecast fields do not show the extensive area of positive anomaly, and in general are not mutually consistent. For 1986, the verifying analysis shows mainly negative anomalies over Europe. There are indications of this over eastern Europe in the two forecast fields, though over central and western Europe, the forecasts are poor. In 1987 and 1988 the 'verifying' rainfall anomalies are more localised. It is arguable whether or not the forecasts show any skill in these years; in any case they are clearly less consistent, in general, than the rainfall forecasts over the monsoon region.

Broadly similar results also hold for the north American region. During years where large-scale rainfall anomalies were observed, the forecasts appeared to show some skill. For example, as discussed in Palmer and Brankovic (1989) some of the 30-day rainfall forecasts during the summers of 1987 of 1988 showed skill, and difference fields between these years captured the essence of the 1988 drought. In this case, Palmer and Brankovic showed that observed sea surface temperature anomalies, which included an intense La Nina

event in the tropical Pacific in 1988, contributed to the intensity of the drought. It is likely that land surface anomalies also played an important role.

6. CONCLUSIONS

We have studied interannual variability in extended-range skill of the ECMWF operational model over a set of monthly forecasts from April 1985 to September 1988. This period was characterised by a number of important changes to the model.

It is found that in the extratropics, the changes in model formulation had a clear impact on the model climate drift. On the other hand, in the tropics, the impact of model changes is less obvious, and forecast errors are apparently strongly dependent on interannual variability in the tropical circulations associated with the El Nino event. It should be pointed out, however, that the model changes were expected to have most effect in the mid-latitudes.

In the first winter of forecasts there was evidence of real skill to day 15 and possibly to day 20 in middle latitudes. On the other hand, for the second and third winter, model skill was confined to the medium range forecast period. There was strong interannual variability in atmospheric predictability , and we found that this was correlated with the tendency of a global version of the Pacific/North American mode in the verifying analyses. We therefore conclude that interannual variability in extended-range skill was not primarily associated with any of the model reformulations.

By contrast, it was shown that there is skill in the prediction of interannual variability in monthly monsoon winds and rainfall, particularly over Africa.

On the other hand it was found that the large tropical systematic error in the model degraded tropical forecast skill significantly to the extent that most of the skill of monthly mean fields was associated with the first 20 days of prediction. The relatively poor skill over India may be associated with its proximity to regions where the model systematic error in large-scale divergent flow was strongest. Skill in the prediction of summertime monthly mean rainfall over Europe was marginal.

For extratropical forecasting, more integrations are needed to establish the reliability of skill out to 15 days. As discussed in III, these integrations should be made in the context of multiple Monte Carlo integrations. On the other hand, for the tropics, multiple integrations are less important. Of more interest would be longer (say seasonal) deterministic integrations with prescribed (observed and persisted) SSTs. The ability to predict seasonal rainfall anomalies with a high resolution NWP model using observed SSTs

would provide important motivation for the development of coupled ocean/atmosphere NWP models for operational seasonal tropical prediction. However, before such development takes place, significant reduction in model biases must be achieved.

REFERENCES

Blondin, C. and H.Böttger, 1987: The surface and sub-surface parametrization scheme in the ECMWF forecasting system: Revision and operational assesment of weather elements. ECMWF Tech.Memo. No.135, 20 pp, ECMWF, Reading, UK.

Brankovic, C.,1989: Systematic errors in deterministic extended-range forecasts. Ph.D. Thesis. University of Zagreb, Yugoslavia, 120pp.

Brankovic C., T.N.Palmer, F.Molteni, S.Tibaldi, and U.Cubasch, 1989: Extended range predictions with ECMWF models: III Time-lagged ensemble forecasting. Submitted to Quart. J. R. Meteor Soc.

Charney, J.G. and J.Shukla, 1981: Predictability of monsoons. In: Monsoon Dynamics, Eds J.Lighthill and R.Pearce. Cambridge University Press, 735 pp.

Datta, R.K. and H.R.Hatwar., 1988: Prediction of monsoon rainfall over India with the ECMWF model. ECMWF Tech.Memo. No.144, 20 pp, ECMWF, Reading, UK.

Dole, R.M., 1986: Persistent anomalies of the extratropical northern hemisphere wintertime circulation: structure. Mon. Wea. Rev., 114, 178-207.

ECMWF, 1988: Reports of the working groups. In: Proceedings of the ECMWF Workshop on Predictability in the medium and extended range, 3-23. ECMWF, Reading, UK.

Ferranti, L., T.N.Palmer, F.Molteni and E.Klinker, 1989: Tropical, extratropical interaction associated with the 30-60 day oscillation, and its impact on mediumnd extended range predictability. Submitted to J. Atmos. Sci.

Folland, C.K., T.N.Palmer and D.E.Parker, 1986: Sahel rainfall and worldwide sea surface temperatures, 1901-85. Nature, 320, 602-607.

Hollingsworth, A., U. Cubasch, S. Tibaldi, C. Brankovic, T.N. Palmer and L. Campbell, 1987: Mid-latitude atmospheric prediction on time scales of 10-30 days. In: Atmospheric and Oceanic Variability, ed. H. Cattle, Royal Meteorological Socieity Monograph, Bracknell, U.K. 117-151.

Jaeger, L., 1976: Monatskarten des Niederschlags für die Ganze Erde. Berichte des Deutschen Wetterdienstes, 139, Band 18.

Lau, N.-C., 1981: A diagnostic study of recurrent meteorological anomalies appearing in a 15-year simulation with a GFDL general circulation model. Mon. Wea. Rev., 109, 2287-2311.

Lu Jingxi and Ding Yihui, 1989: Climatic study on the summer tropical easterly jet at 200 hPa. Adv. Atmos. Sci., 6, 215-226.

Manabe, S. and D.G.Hahn, 1981: Simulation of atmospheric variability. Mon. Wea. Rev. 109, 2260-2286.

Miller, M.J., T.N.Palmer and R.Swinbank, 1989: Parametrization and influence of subgridscale orography in general circulation and numerical weather prediction models. Meteorol. Atmos. Phys., 40, 84-109.

Miller, M.J., 1988: The sensitivity of systematic errors of the ECMWF forecast model to parametrized processes. In CAS/JSC working group on numerical experimentation, Report no.12, 'Workshop on systematic errors in models of the atmosphere', WMO/TD No.273, 289-296.

Molteni F., S.Tibaldi, and T.N.Palmer, 1989: Regimes in the wintertime circulation over northern extratropics: I Observational evidence. Quart. J. R. Meteor. Soc. To appear.

Molteni F. and S.Tibaldi, 1989: Regimes in the wintertime circulation over northern extratropics: II Consequences on dynamical predictability. Submitted to Quart. J. R. Meteor. Soc.

Newell, R.E. and J.W.Kidson, 1984: African mean wind changes bewteen Sahelian wet and dry periods. J. Climat., 4, 27-33.

Owen, J.A. and C.K.Folland, 1988: Modelling the influence of sea surface temperatures on tropical rainfall. In: Recent climate change - a regional approach. Ed S.Gregory, Belhaven Press, London.

Palmer, T.N., 1986: Influence of the Atlantic, Pacific, and Indian Oceans on Sahel rainfall. Nature, 322, 251-253.

Palmer, T.N., 1987: Modelling low-frequency variability of the atmosphere. In 'Atmospheric and oceanic variability', ed. H. Cattle, Royal Meteorological Society, Bracknell, 75-103.

Palmer, T.N., 1988: Medium and extended range predictability and stability of the Pacific/North American mode. Quart. J. R. Meteor. Soc., 114, 691-714.

Palmer, T.N. and D.A.Mansfield, 1986: A study of wintertime circulation anomalies during past El Nino events, using a high resolution general circulation model: I Influece of climatology. Quart. J. R. Meteor. Soc. 112, 639-660.

Palmer, T.N. and C.Brankovic, 1989: The 1988 US drought linked to anomalous sea surface temperature. Nature, 338, 54-57.

Saha, S., and H.M. van den Dool, 1988: A measure of the practical limit of predictability. Mon.Wea.Rev., 116, 2522-2526.

Shukla, J., D.A.Mooley and D.A.Paolino, 1988: Long-range forecasting of summer monsoon rainfall over India. Pontificae Academiae Scientiarum Scripta Varia, 69, 147-178.

Simmons, A.J., 1987: Orography and the development of the ECMWF forecast model. In: Proceedings of the 1986 ECMWF Seminar on observation, theory and modelling of orographic effects, ECMWF, Reading, UK, Vol.2, 129-163.

Simmons, A.J., D.M.Burridge, M.Jarraud, C.Girard, and W.Wergen., 1989: The ECMWF medium-range prediction models: Development of the numerical formulations and the impact of increased resolution. Meteorol. Atmos. Phys., 40, 28-60.

Tibaldi, S., T.N.Palmer, C.Brankovic, and U.Cubasch, 1989: Extended range predictions with ECMWF models: II Influence of horizontal resolution on systematic error and forecast skill. Submitted to Quart. J. R. Meteor. Soc.

Tiedtke, M., W.A. Heckley and J. Slingo, 1988: Tropical forecasting at ECMWF: The influence of physical parametrization on the mean structure of forecasts and analyses. Quart.J.R.Meteor.Soc., 114, 639-664.

Wallace, J.M. and D.S.Gutzler, 1981: Teleconnections in the geopotential height field during the northern winter. Mon. Wea. Rev., 109, 784-812.

Wallace, J.M., S.Tibaldi and A.J.Simmons, 1983: Reduction of systematic forecast errors in the ECMWF model through the introduction of an envelope orography. Quart. J. R. Meteor. Soc., 109, 683-717.

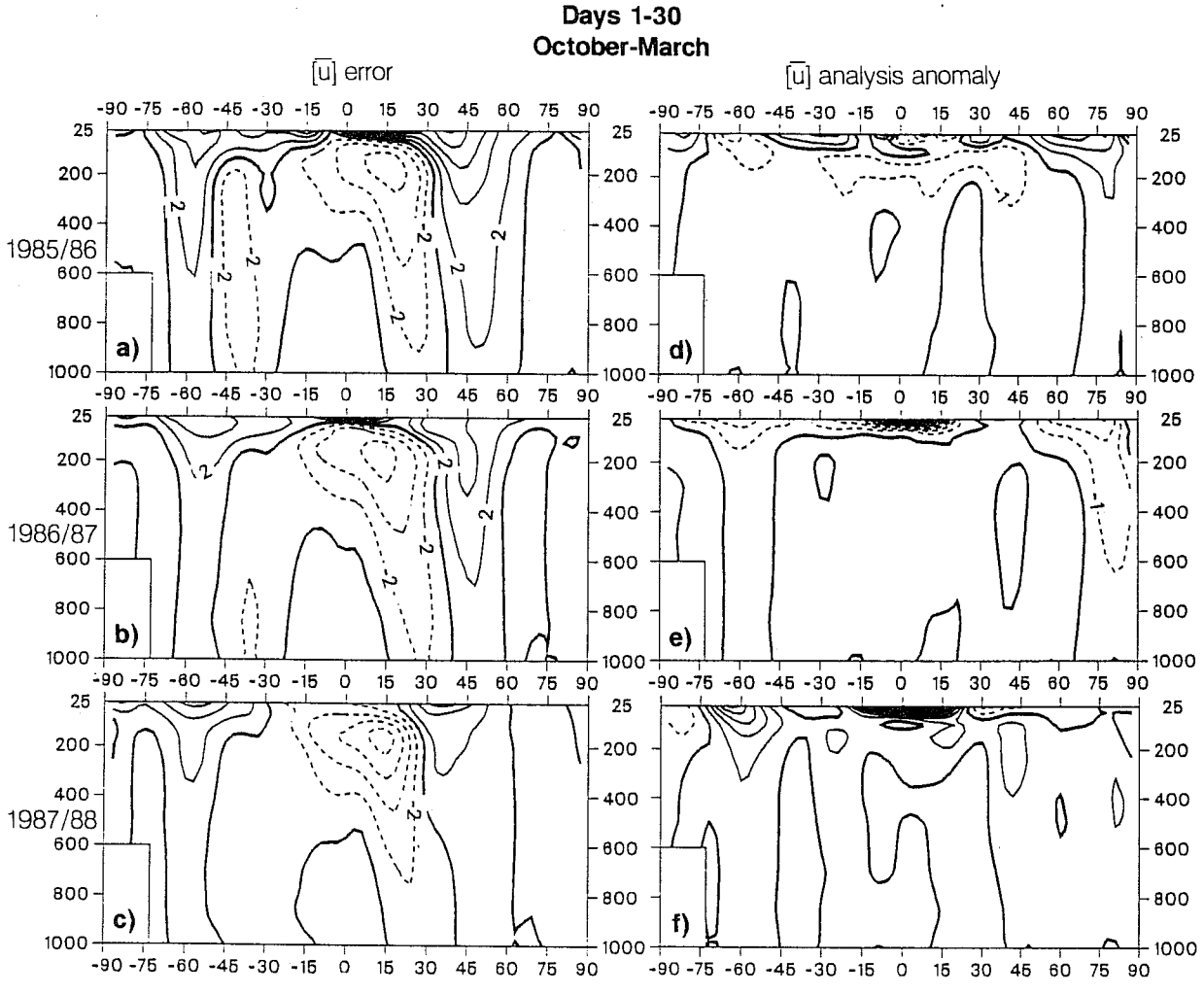

Fig.1 30-day mean zonal mean zonal wind averaged over the October - March forecast periods a) forecast error for 1985/86. b) forecast error for 1986/87. c) forecast error for 1987/88. d) analysis anomaly for 1985/86. e) analysis anomaly for 1986/87. f) analysis anomlaly for 1987/88. ntour interval for a)-c) 2 m/s, d)-f) 1 m/s.

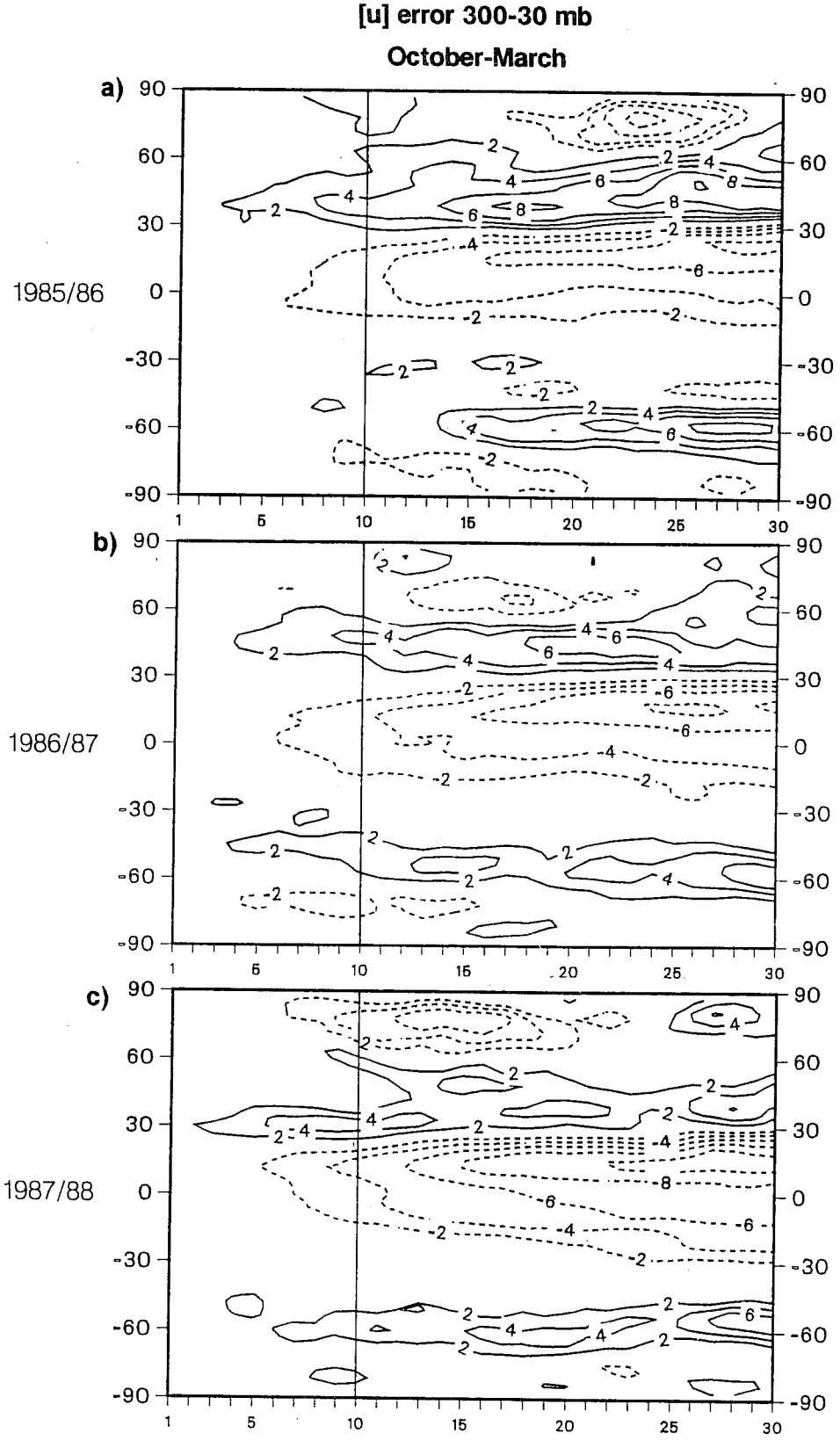

Fig 2. Latitude-time diagrams of zonal mean wind error averaged between 300-30mb for October to March forecasts.a) 1985/86. b) 1986/87. c) 1987/88. Contours every 2 m/s.

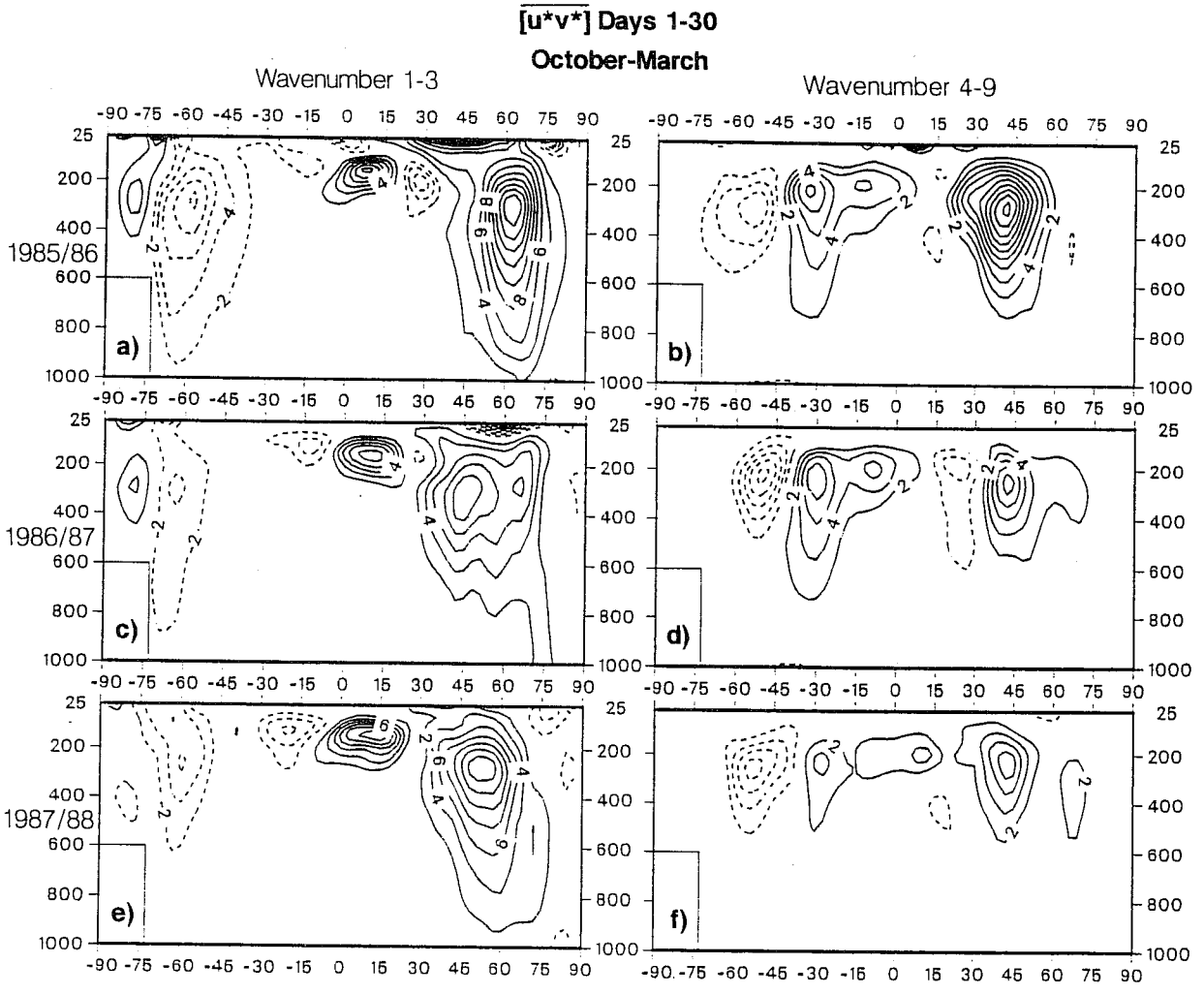

Fig.3 30-day mean zonal cross section of horizontal momentum flux error. Mean of October to March forecasts. Left: contribution from zonal waves 1-3. Right: contribution from zonal waves 4-9. a), b) 1985/86; c), d) 1986/87; e), f) 1987/88. Contours every 2m2/s2.

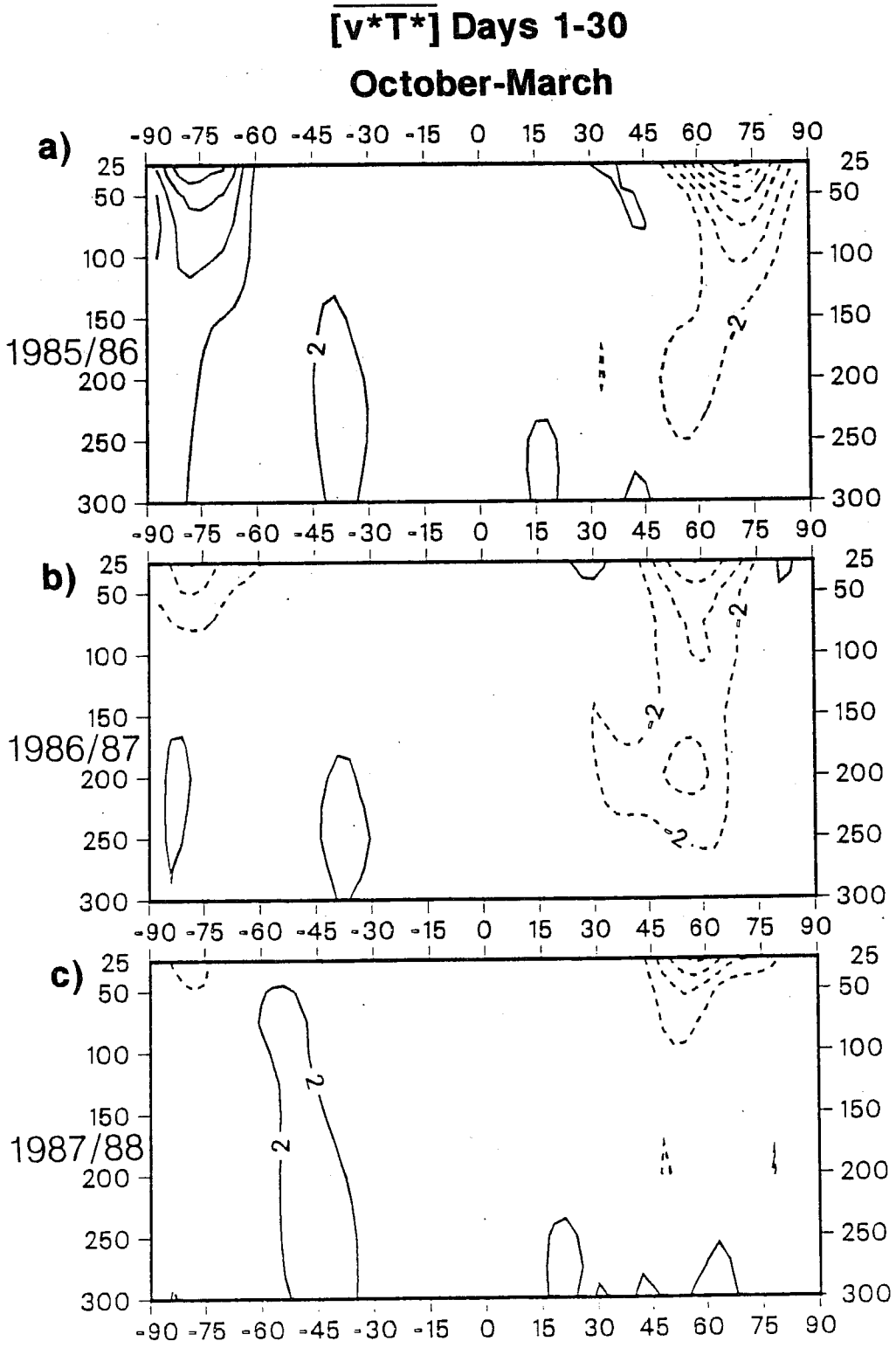

Fig.4 30-day mean zonal mean cross sections of horizontal heat flux error. Mean of October to March forecasts. a) 1985/86; b) 1986/87; c) 1987/88. Contours every 2 K m/s.

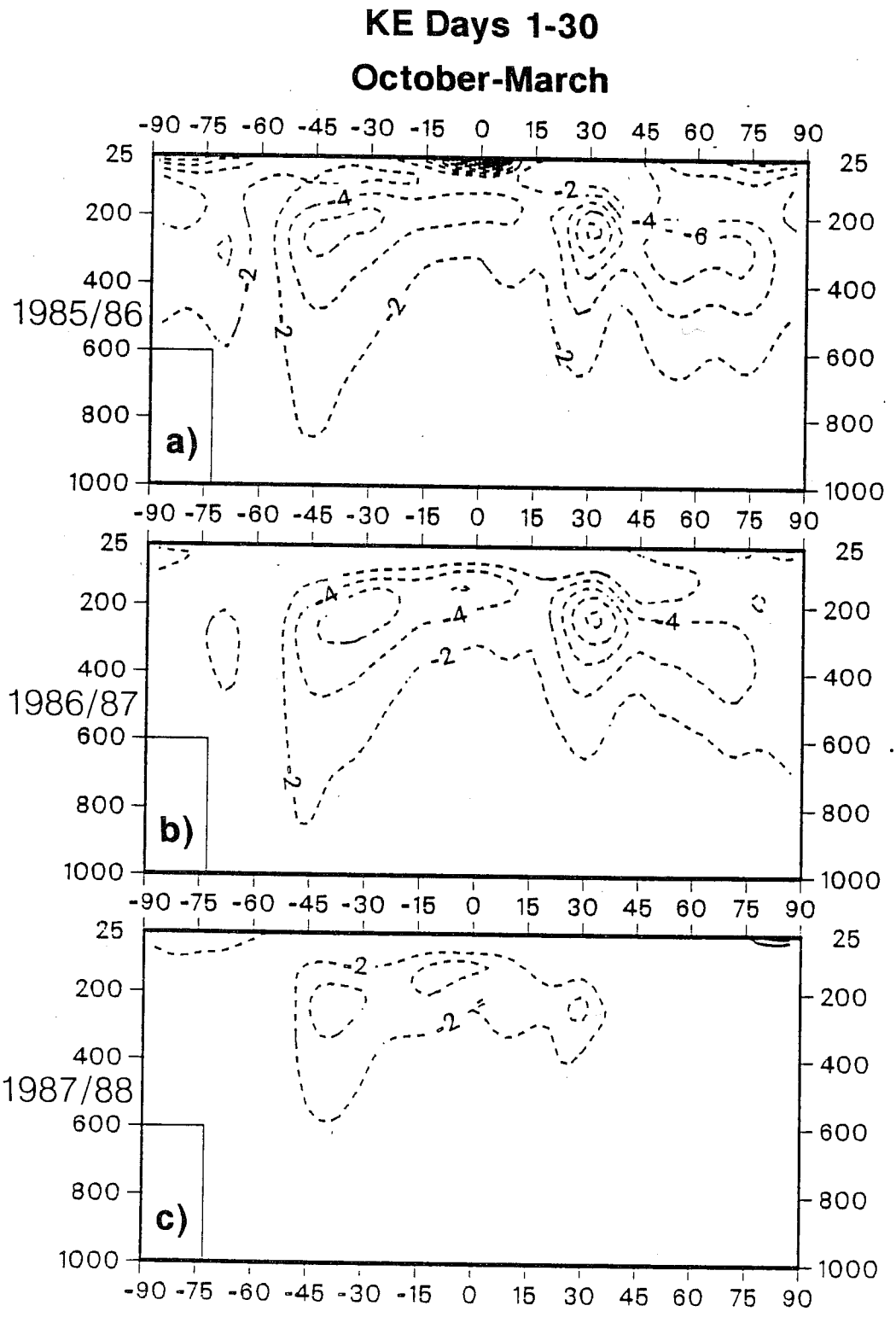

Fig.5 30-day mean zonal mean cross sections of error in eddy kinetic energy. Mean of October to March forecasts. a) 1985/86; b) 1986/87; c) 1987/88. Contours every 2 kJ/m2.

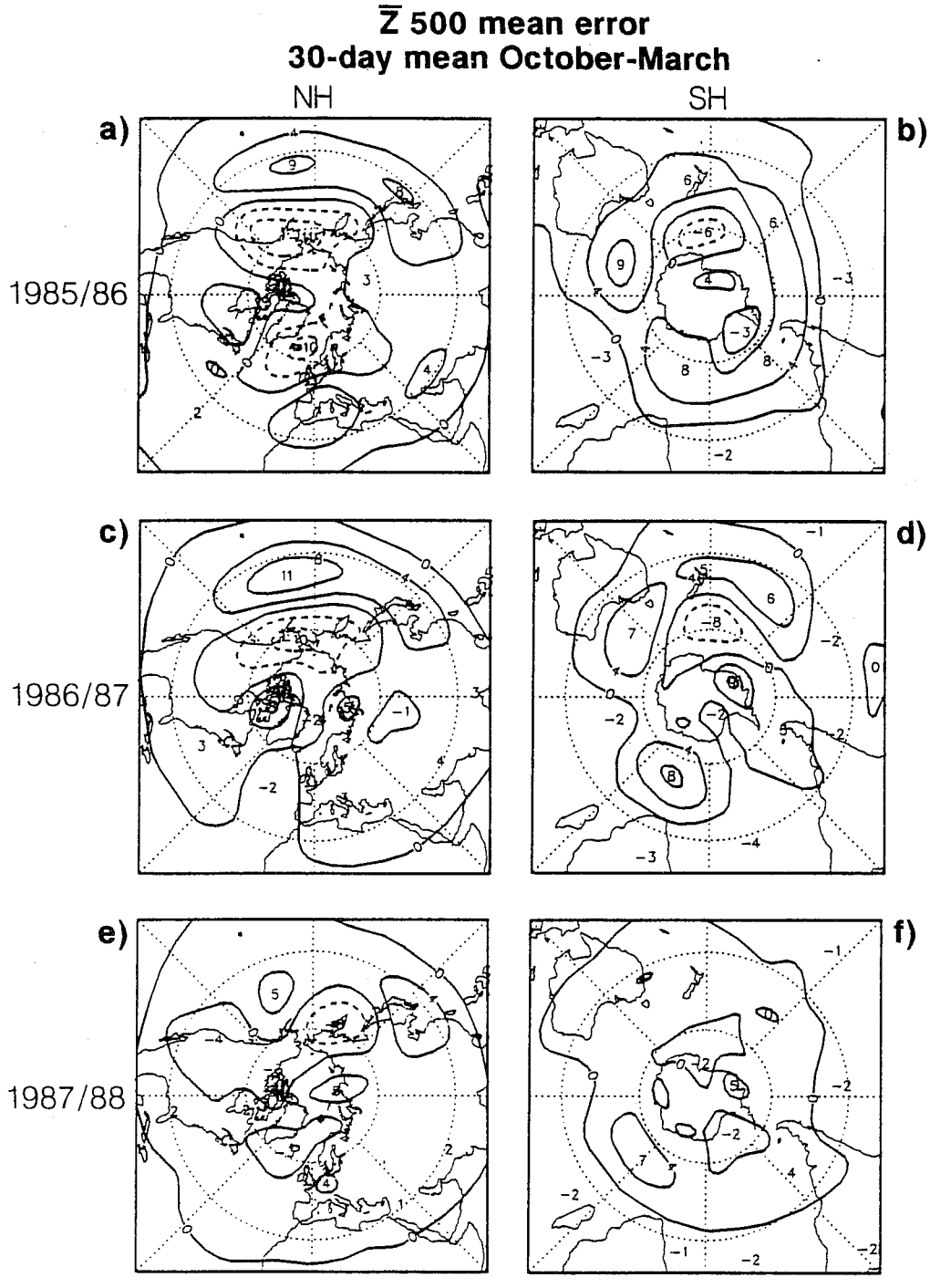

Fig.6 30-day mean error of 500mb geopotential height. Mean of October to March forecasts. Left: northern hemisphere; right: southern hemisphere. a), b) 1985/86; c), d) 1986/87; e), f) 1987/88. Contours every 4 dam.

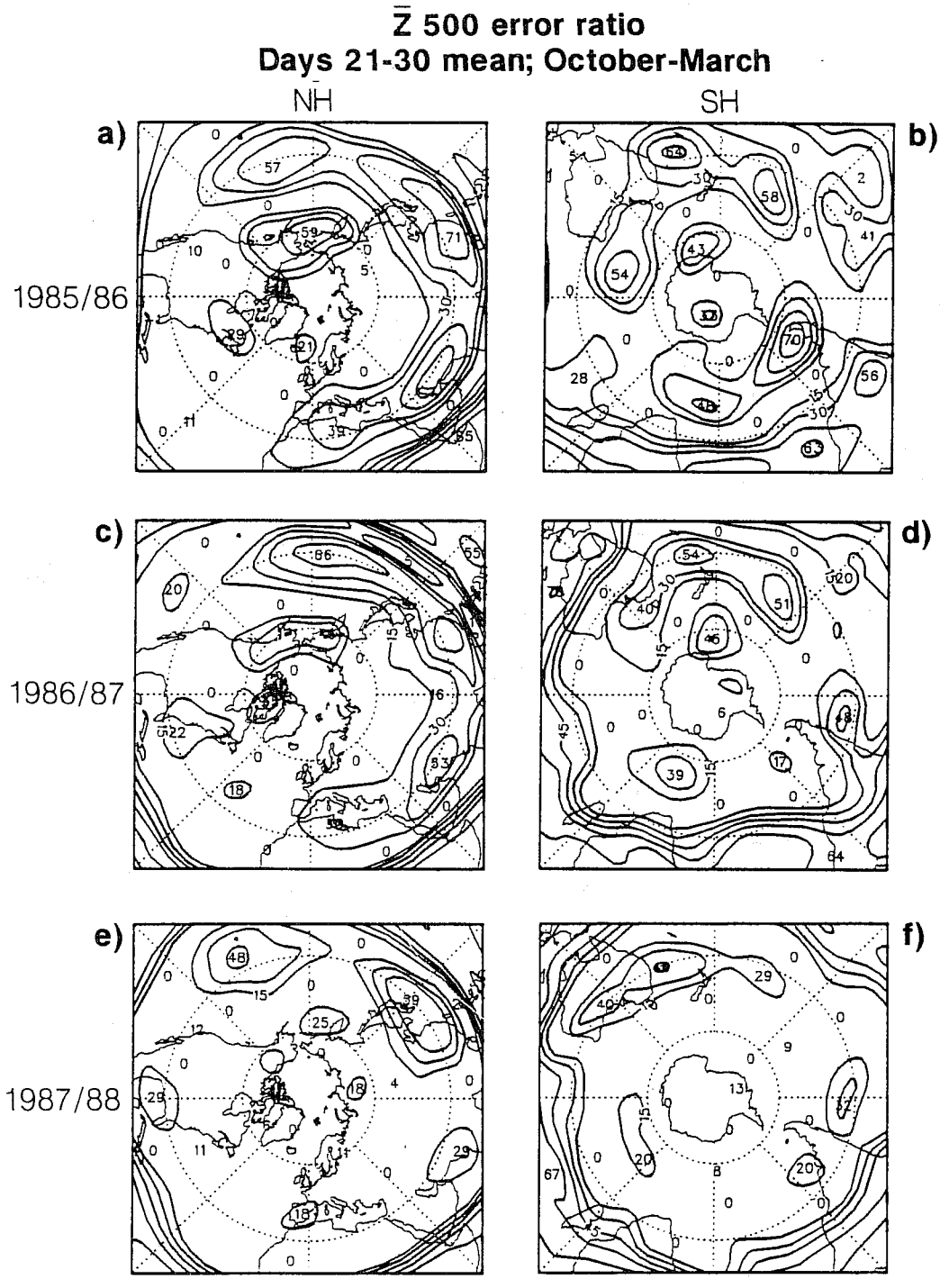

Fig.7 Ratio of systematic to total daily mean square error of 500 mb geopotential height in extratropics. Computed using days 21-30 of October to March forecasts. Left: northern hemisphere; right: southern hemisphere. a), b) 1985/86; c), d) 1986/87; e), f) 1987/88. Contours every 15%.

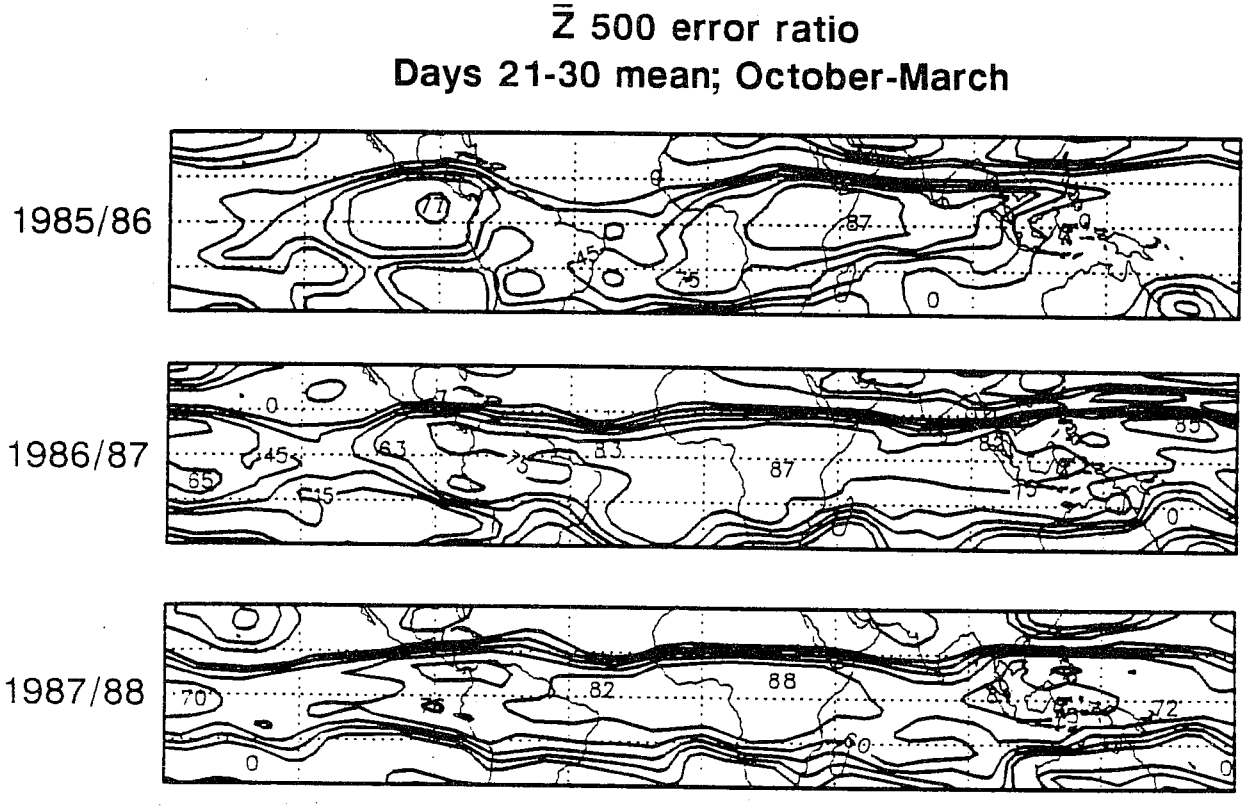

Fig.8 As Fig 7 but for tropics. a) 1985/86; b) 1986/87; c) 1987/88.

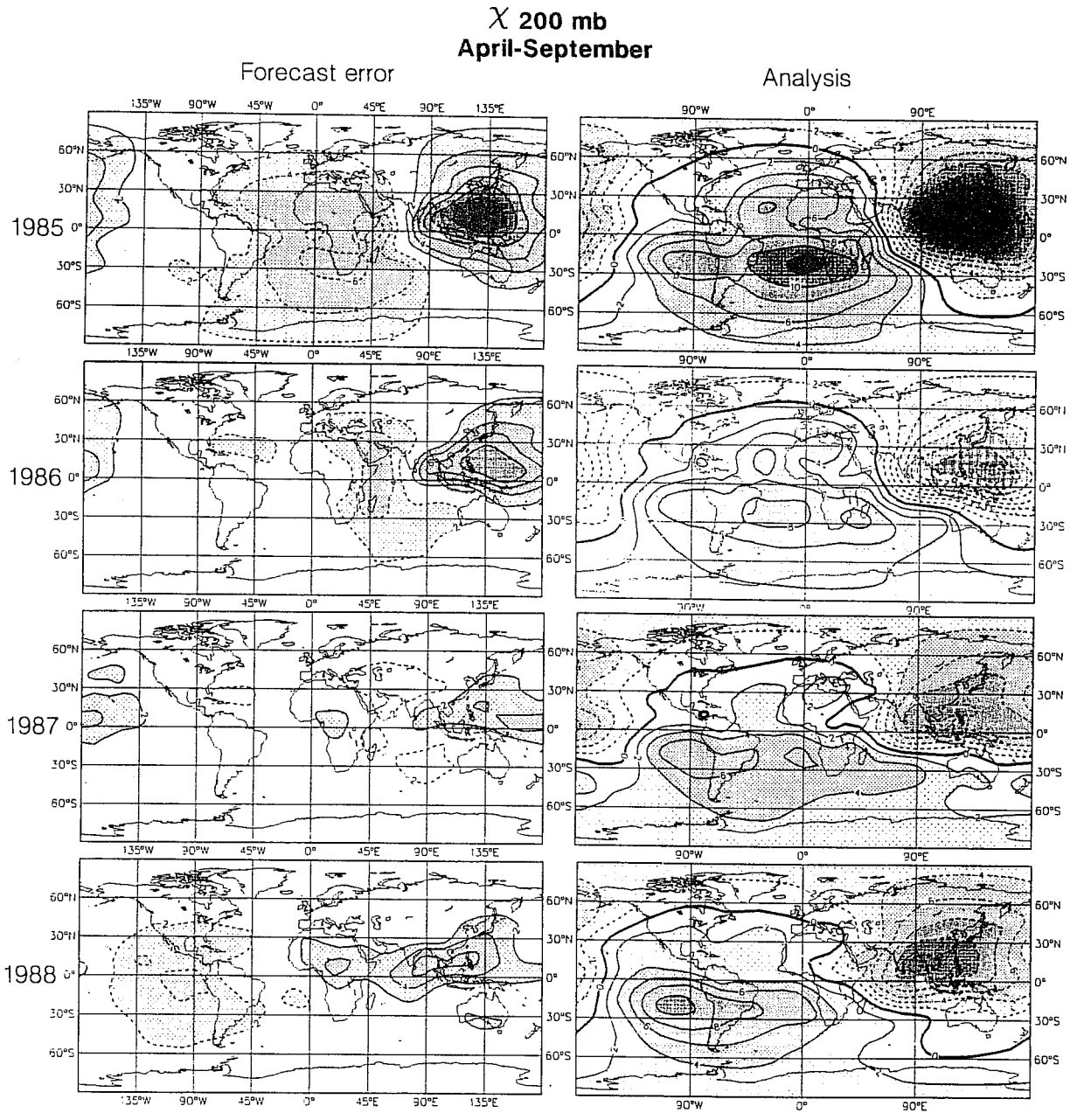

Fig.9 Mean April to September 30-day mean 200 mb velocity potential. Left: forecast error; right; verifying analysis. Top to bottom: years 1985, 1986, 1987 and 1988. Contours every 2 x 10-6 s-1 for error and 4 x 10-6 s-1 for analyses.

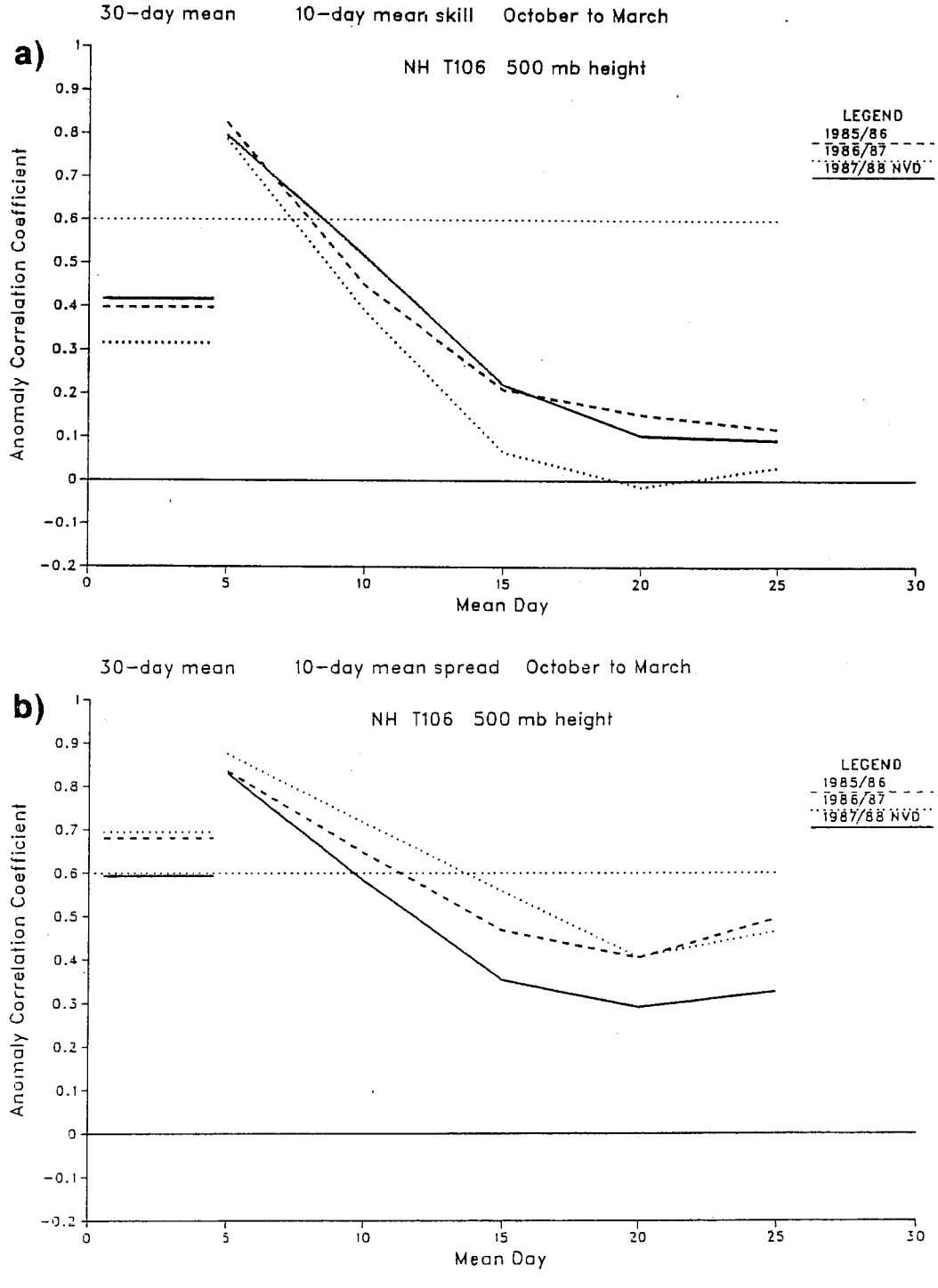

Fig.10 10-day and 30-day mean northern hemisphere 500 mb height anomaly correlation coefficients for: a) model skill; b) spread (between adjacent forecasts for the October to March period). Dashed: 1985/86; dotted: 1986/87; solid: 1987/88.

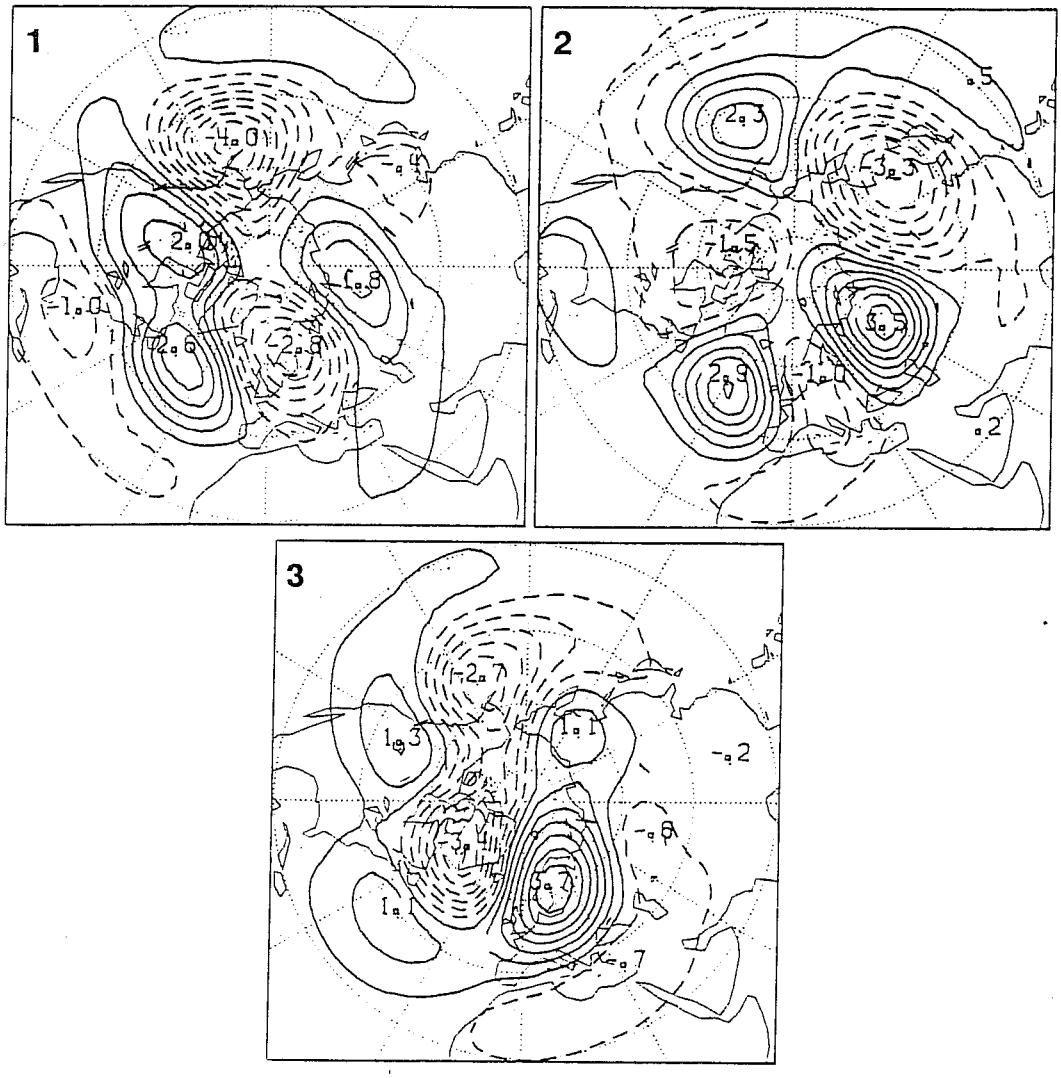

Fig.11 Three orthogonal rotated EOFs of 500mb height anomaly (departure from zonal mean). The space spanned by these EOFs contains the 6 principal local density maxima (clusters) found by Molteni at al (1989) from a study of 5-day mean wintertime fields in a larger dimensional phase space. Contours every 0.5 from +0.25 (-0.25); zero contour not drawn.

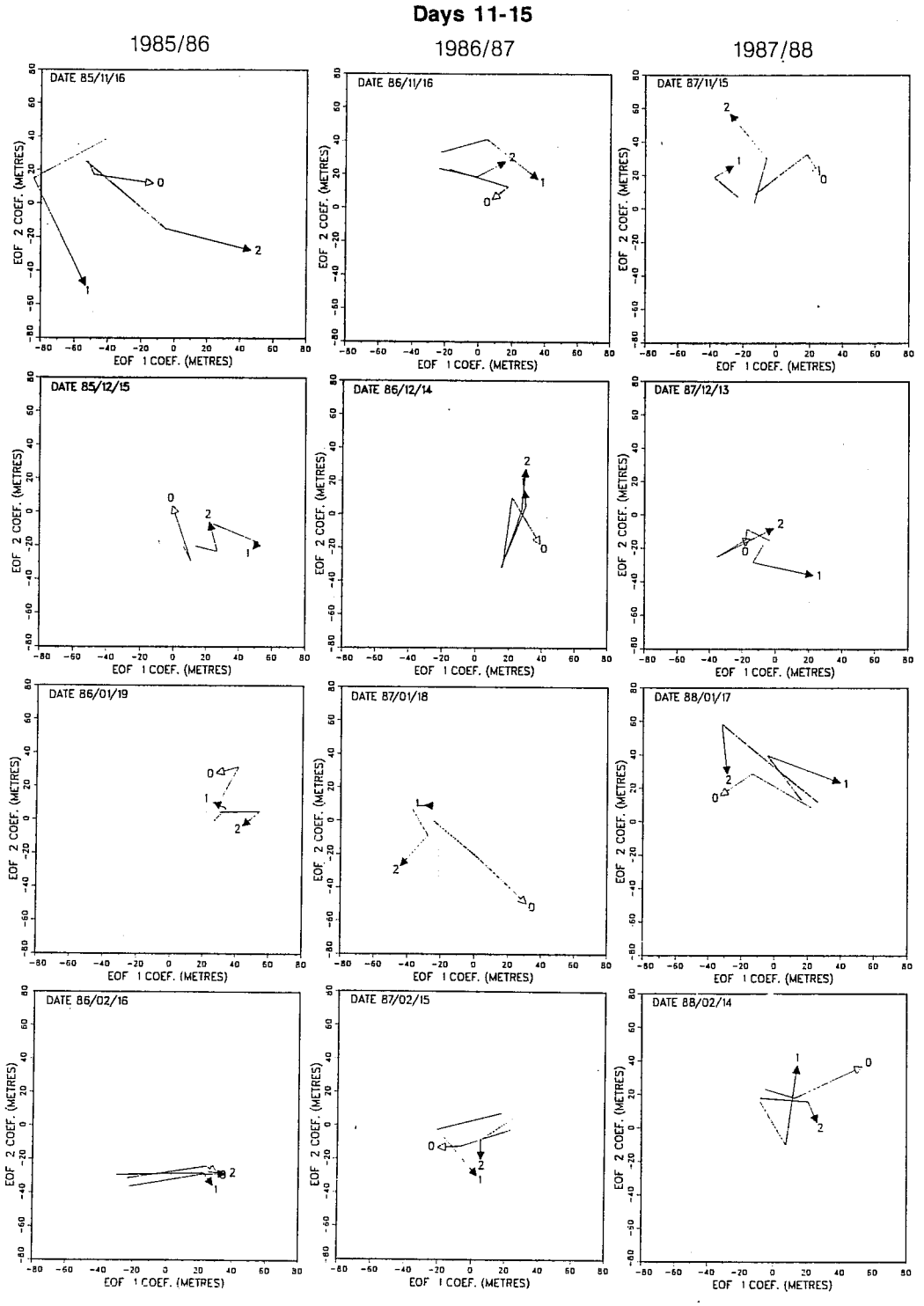

Fig.12 Phase space trajectories of twin forecasts (numbered '1' and '2'), and verifying analysis (numbered zero) from the wintertime period (November to February inclusive) Line segments join values for the 5-day mean fields 1-5, 6-10, and 11-15. Left hand column: 1985/86. Middle column: 1986/87. Right hand column: 1987/88.

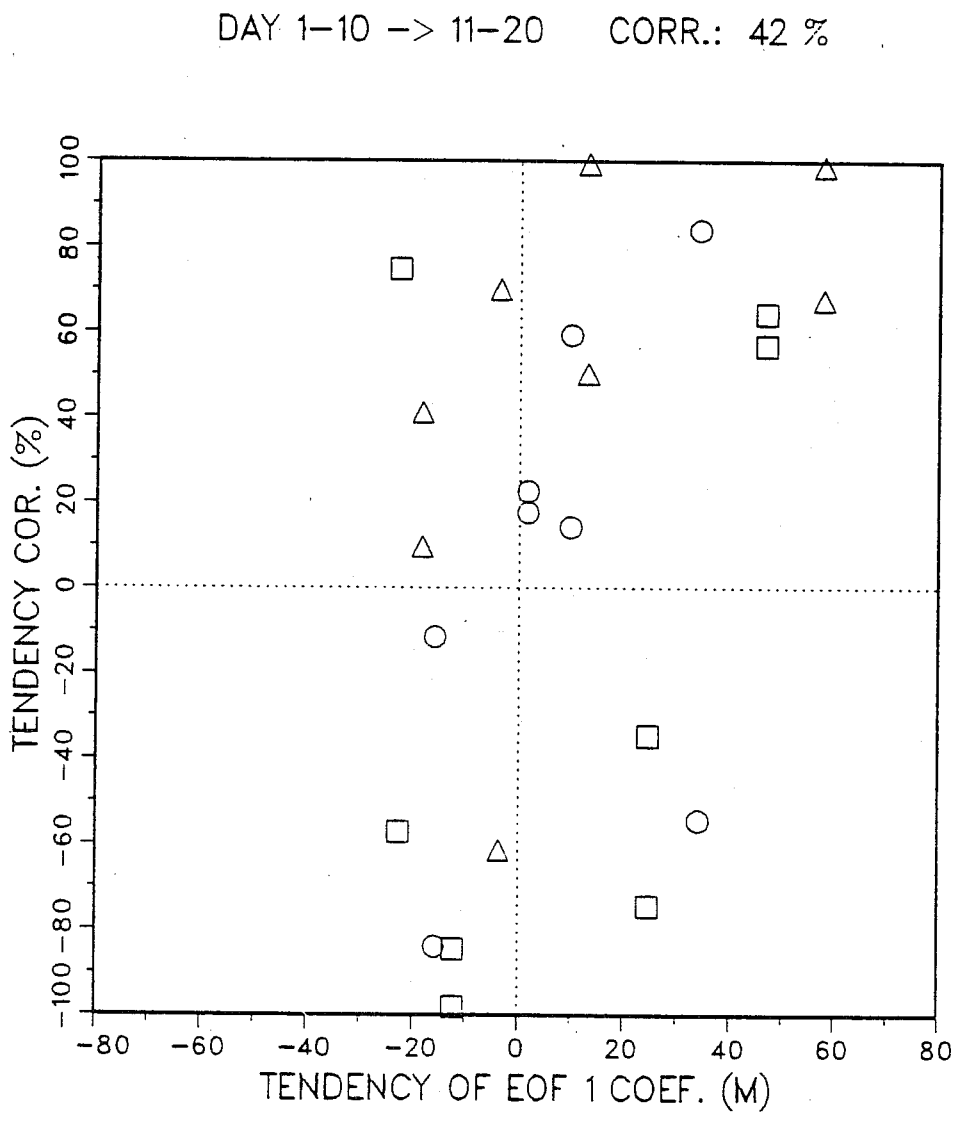

Fig.13 Scatter diagram showing the correlation between the tendency correlation (TC) coefficient skill score between day 1-10 and day 11-20, and the tendency between days 1-10 and 11-20 of the observed value of rotated EOF1. Triangle markers denote forecasts from the winter 1985/86; circle markers denote forecasts from the winter 1986/87; square markers denote forecasts from the winter 1987/88.

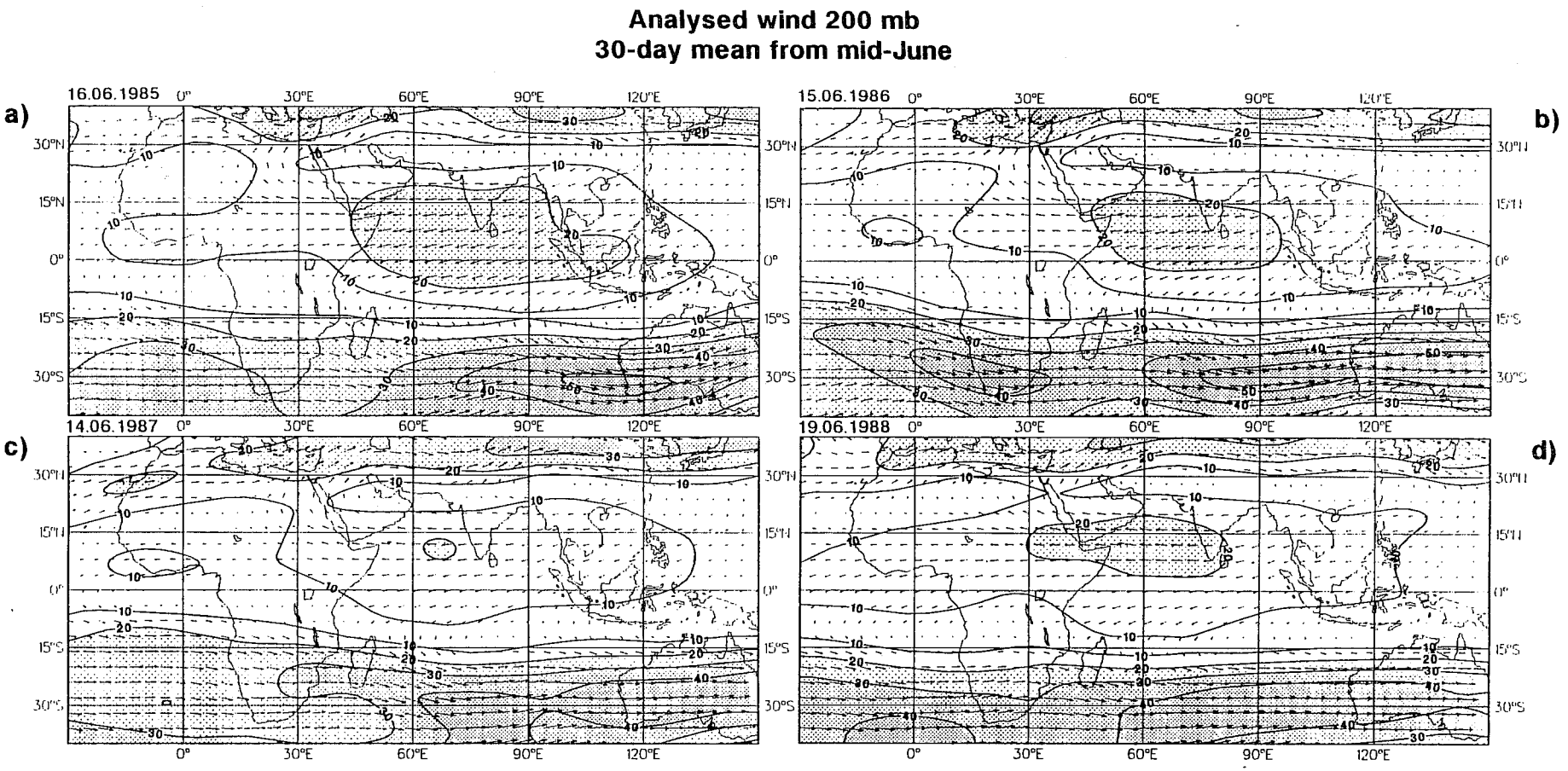

Fig.14 Analysis of 200 mb wind (m/s) averaged over 30 days from: a) 16 June 1985, b) 15 June 1986, c) 14 June 1987, d) 19 June 1988. Stippled area shows wind speeds greater than 20 m/s.

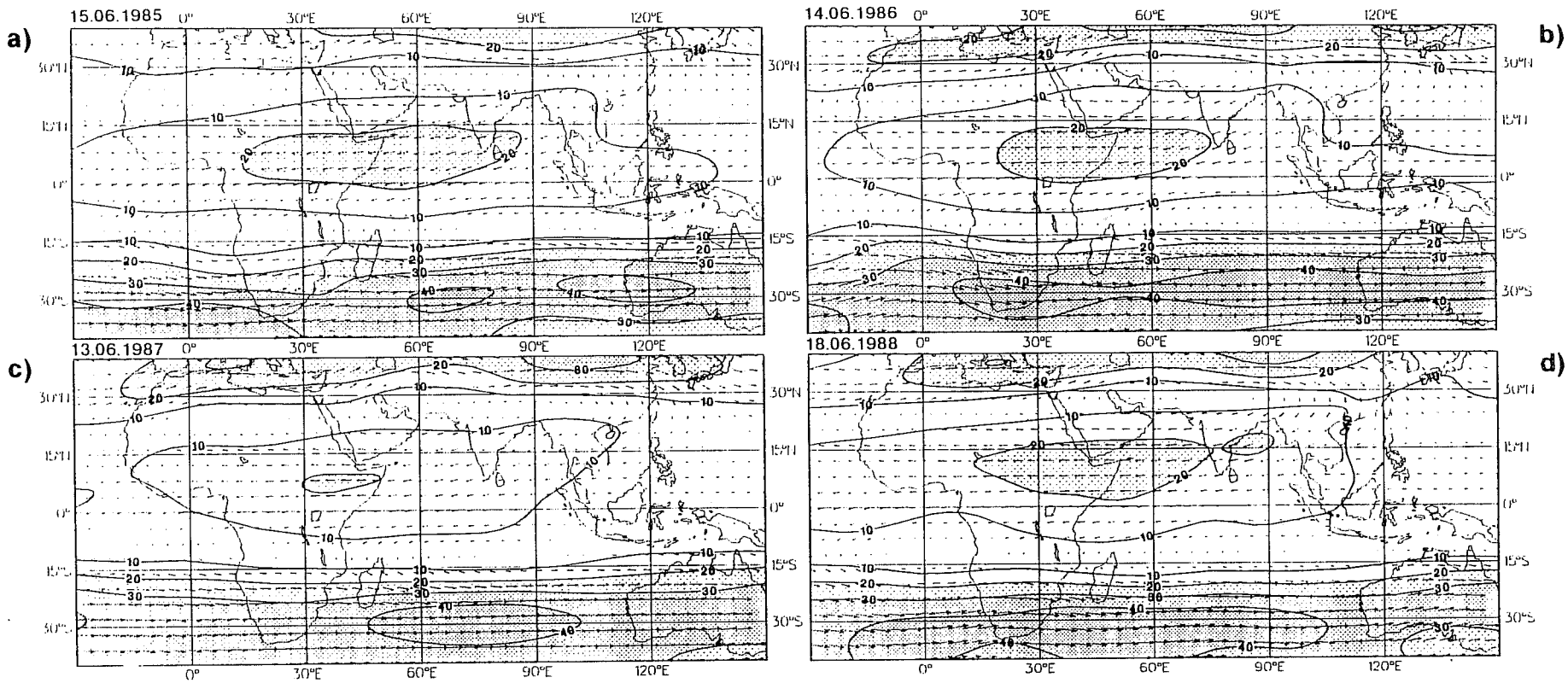

Fig.15 30-day mean prediction of 200 mb wind (m/s) from forecast initialised on a) 15 June 1985, b) 14 June 1986, c) 13 June 1987, d) 18 June 1988. Stippled area shows wind speeds greater than 20 m/s.

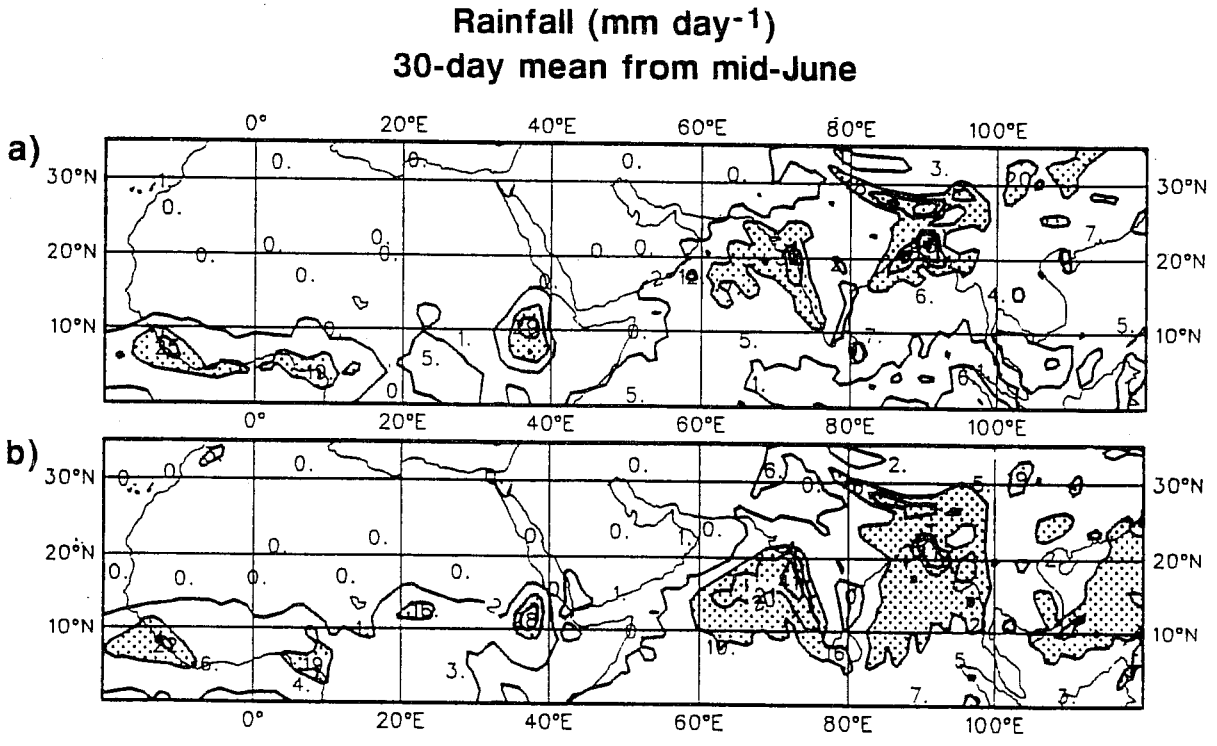

Fig.16 a) 30-day mean simulated rainfall (mm/day), averaged over 8 T106 forecasts from mid June; b) 24 hr accumulated rainfall (mm/day) averaged over the period for which the T106 forecasts in a) verify.

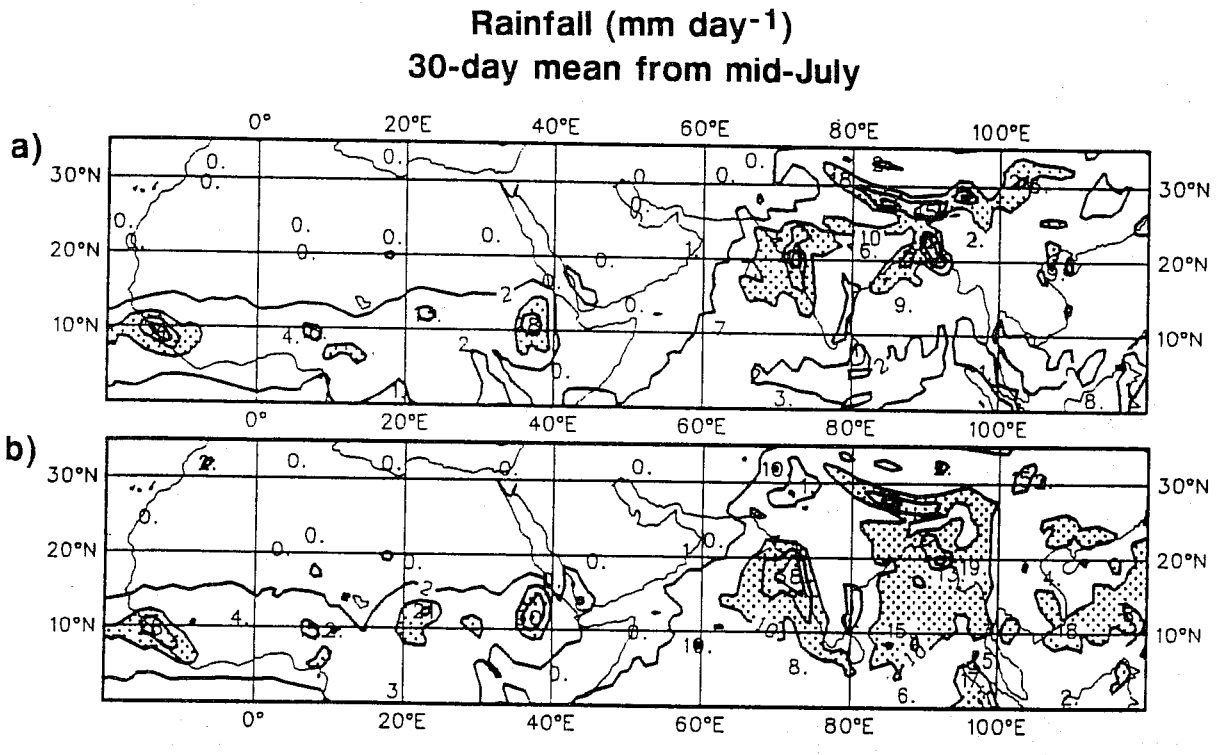

Fig.17 As Fig.16 but for forecasts from mid July.

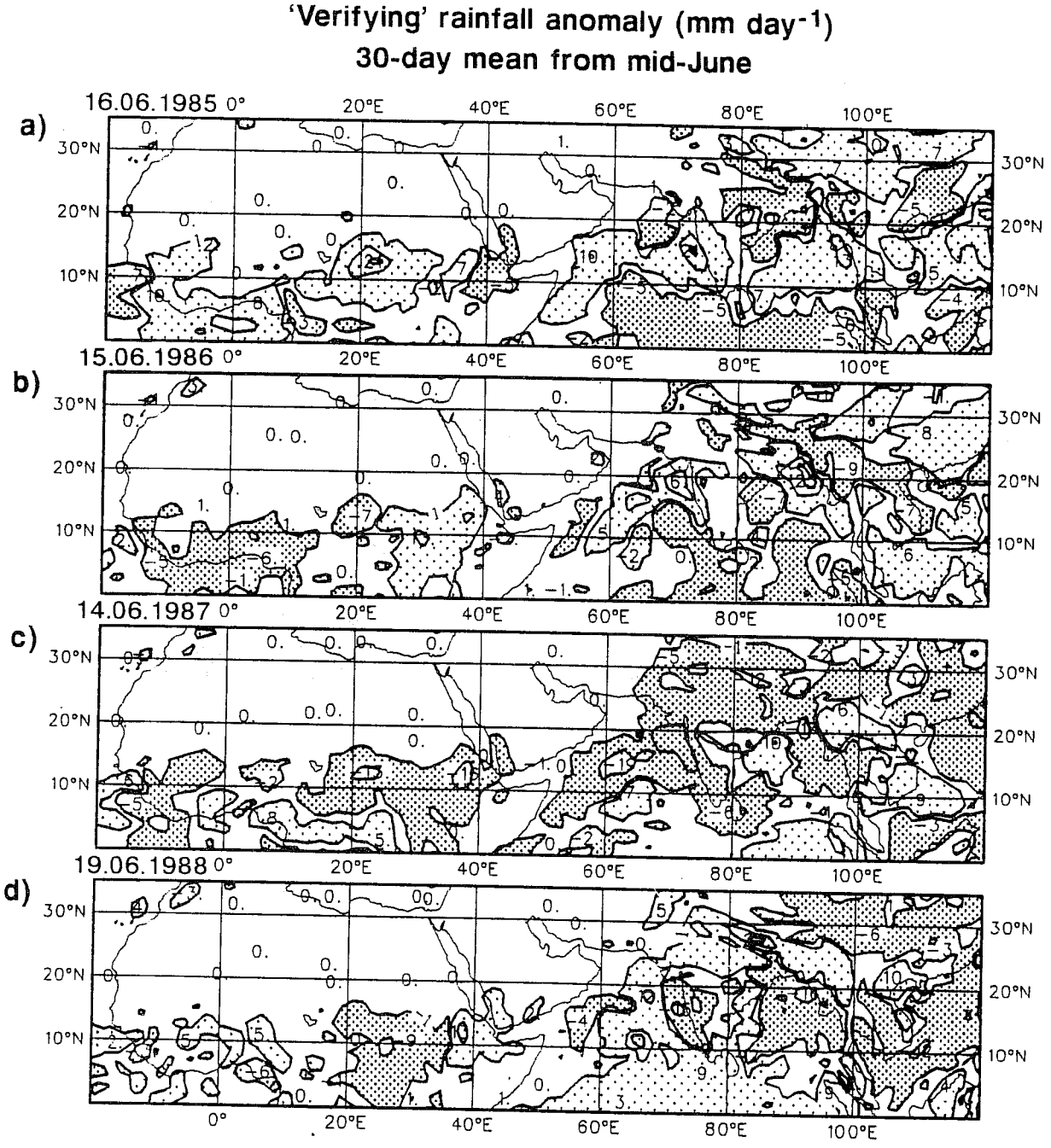

Fig.18 Mean 24 hr accumulated rainfall anomalies in mm/day (departure from Fig.16b) for each 30-day verifying period from mid June to mid July.

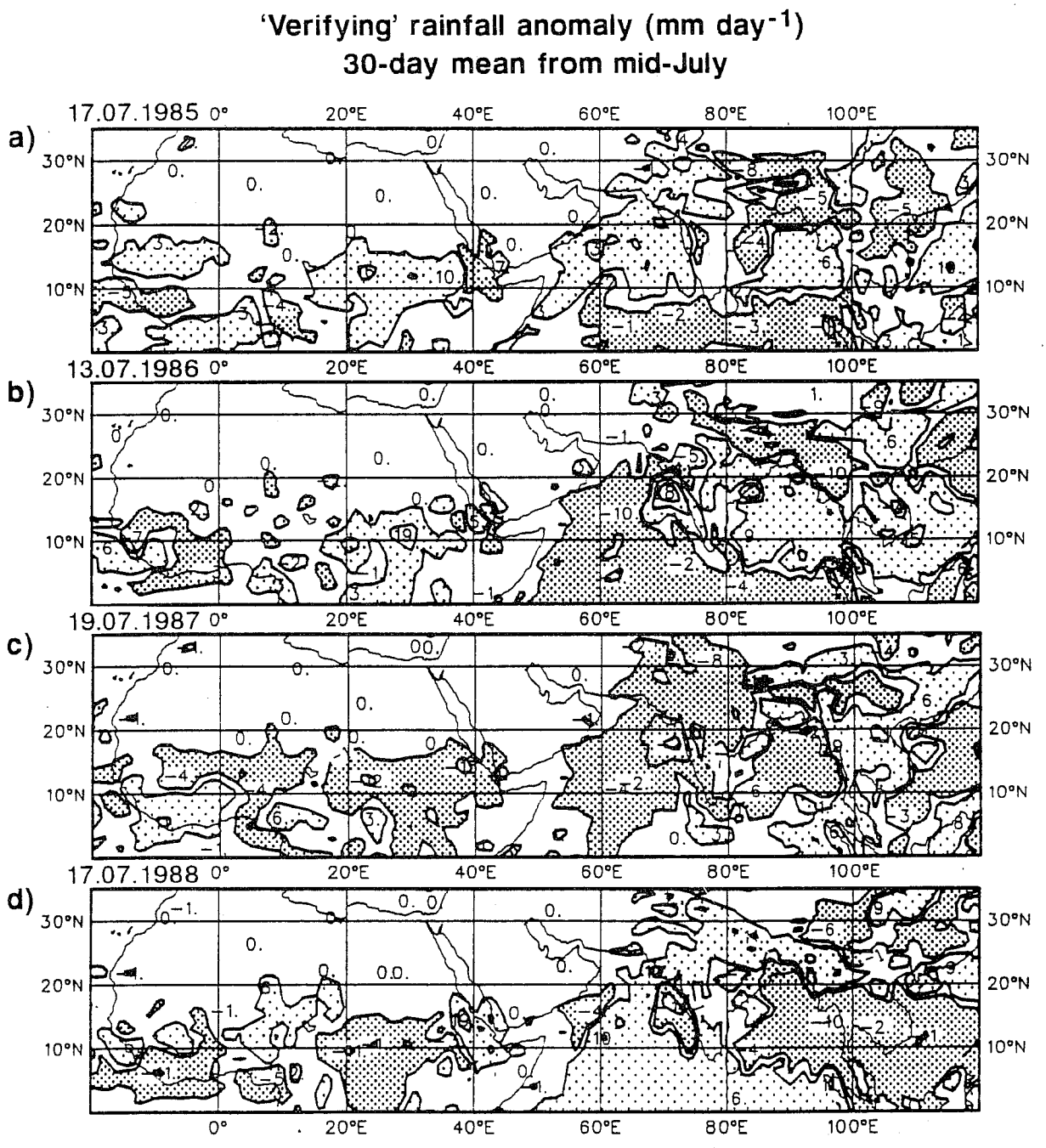

Fig.19 As Fig.18 but for mid July.

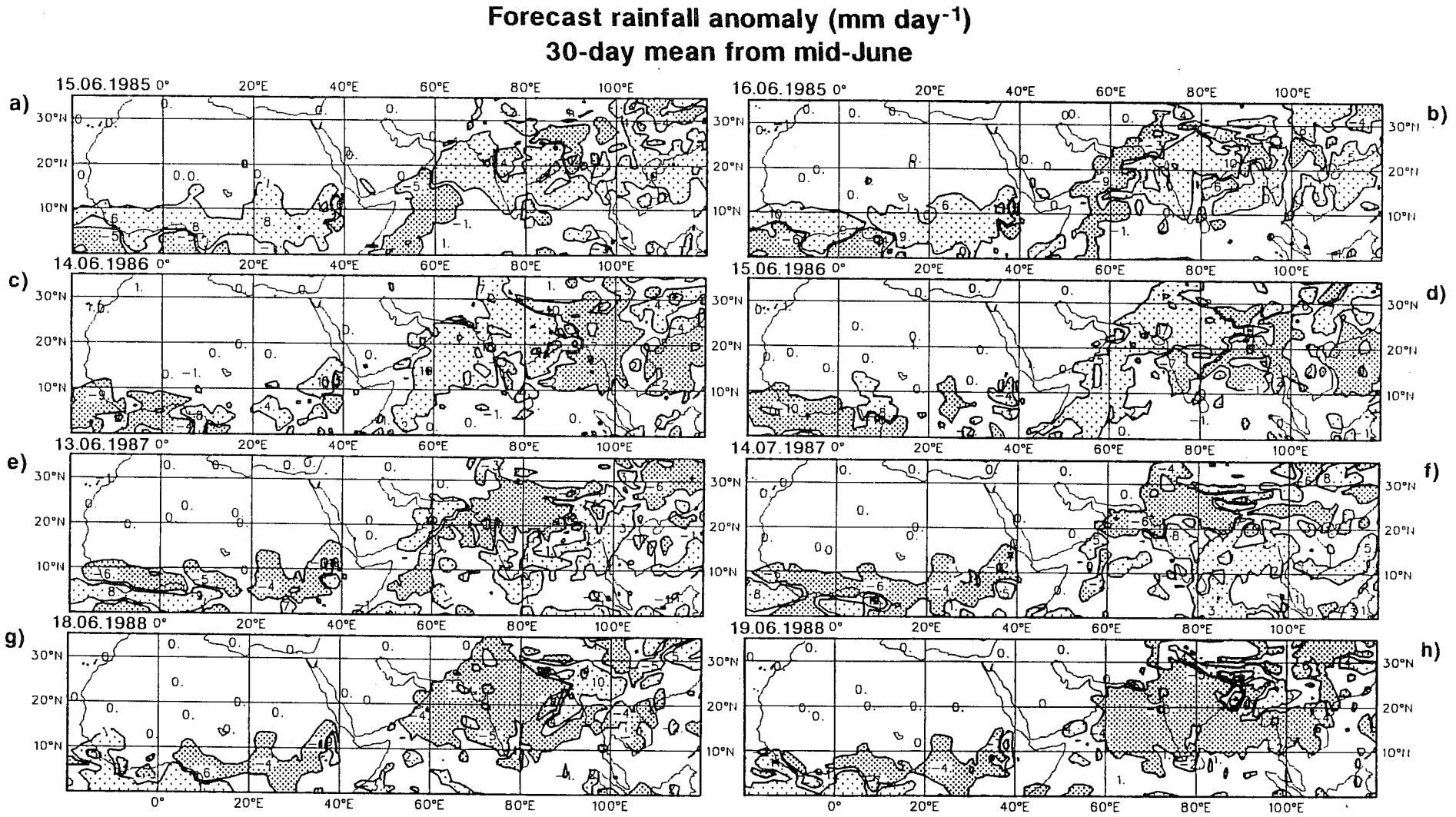

Fig.20 30-day mean forecast anomaly in mm/day (departure from Fig.16a) for each T106 forecast from mid June.

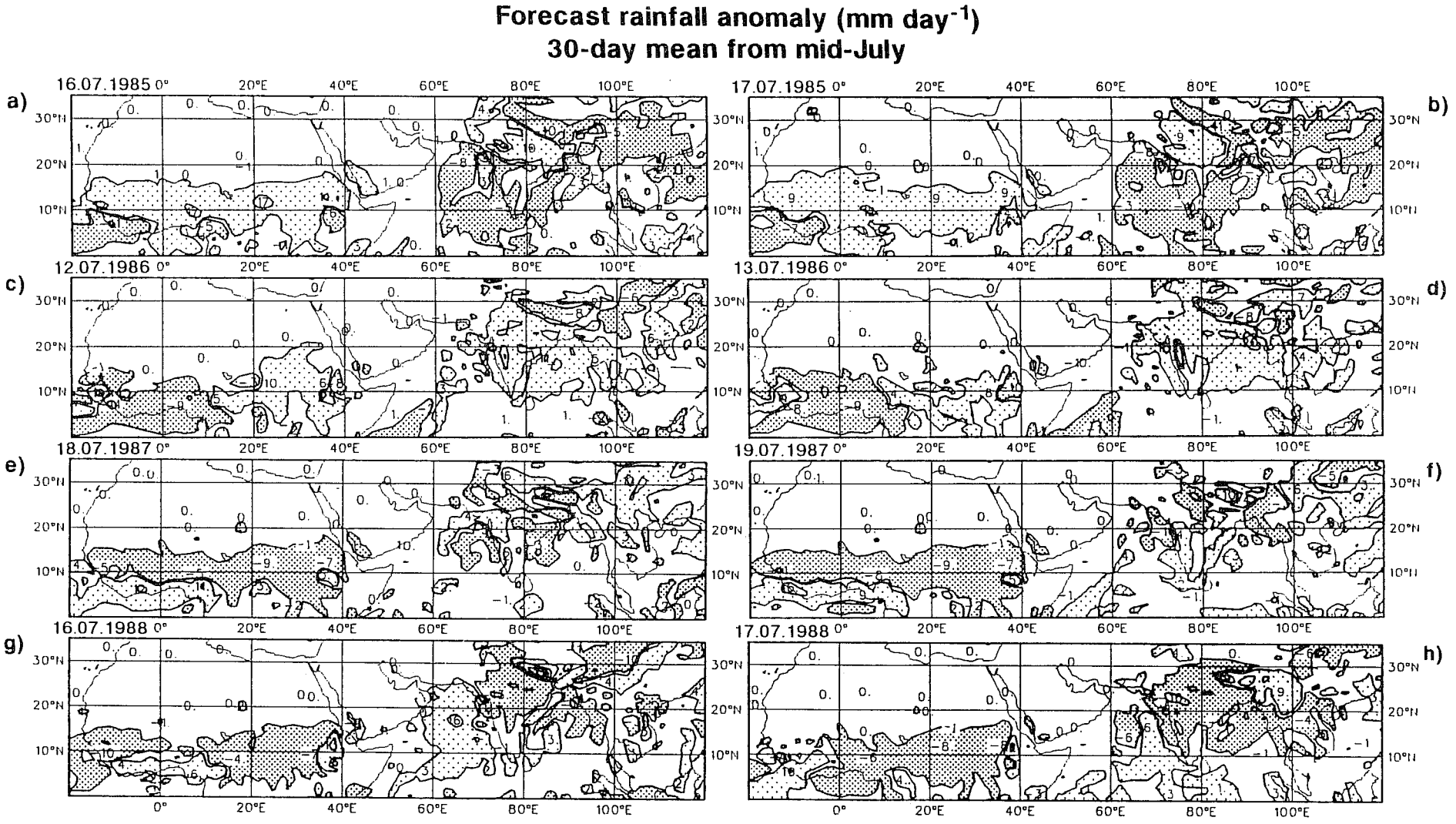

Fig.21 As Fig.20 but for mid July.

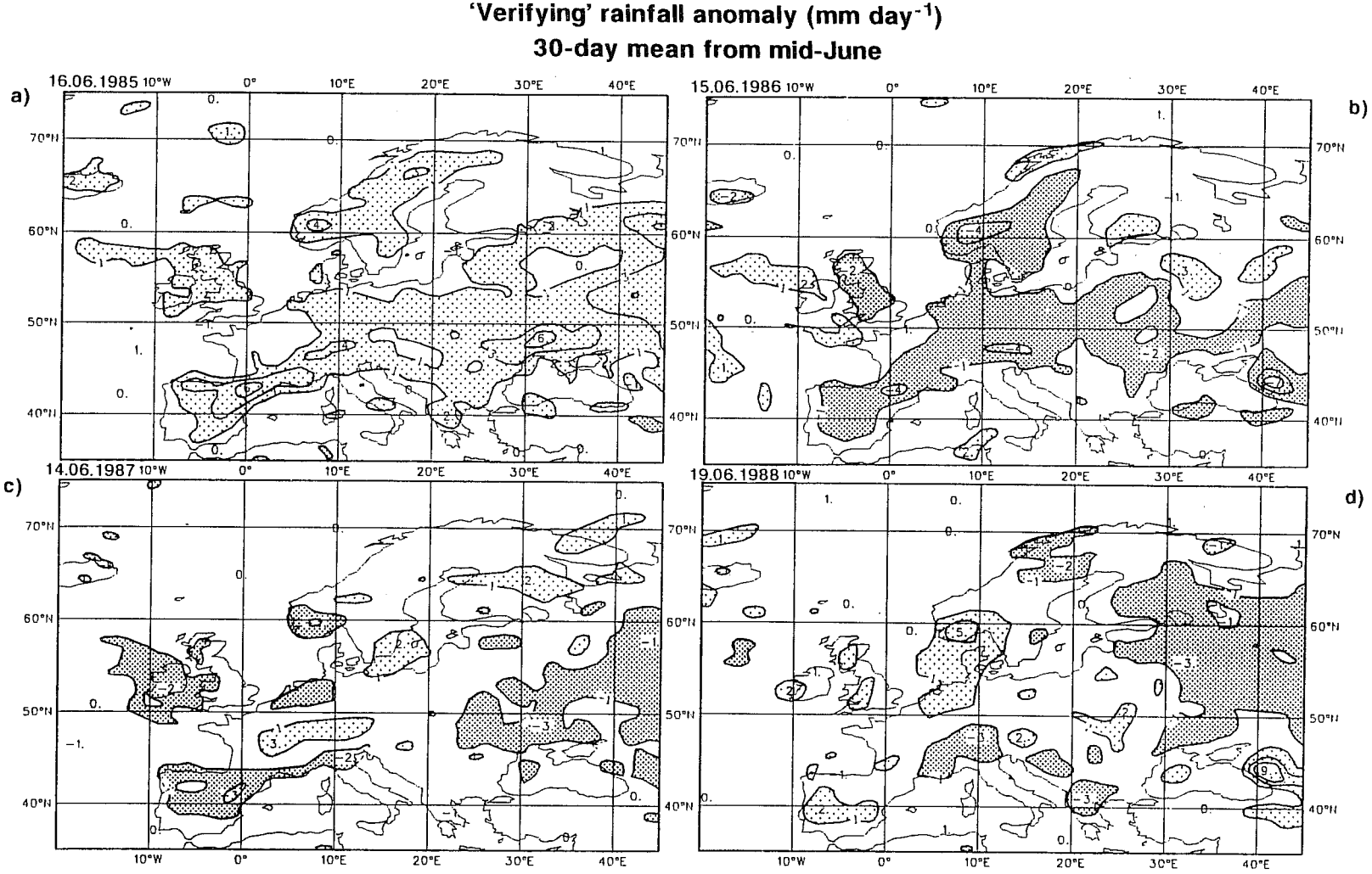

Fig.22 As Fig.18 but for European region.

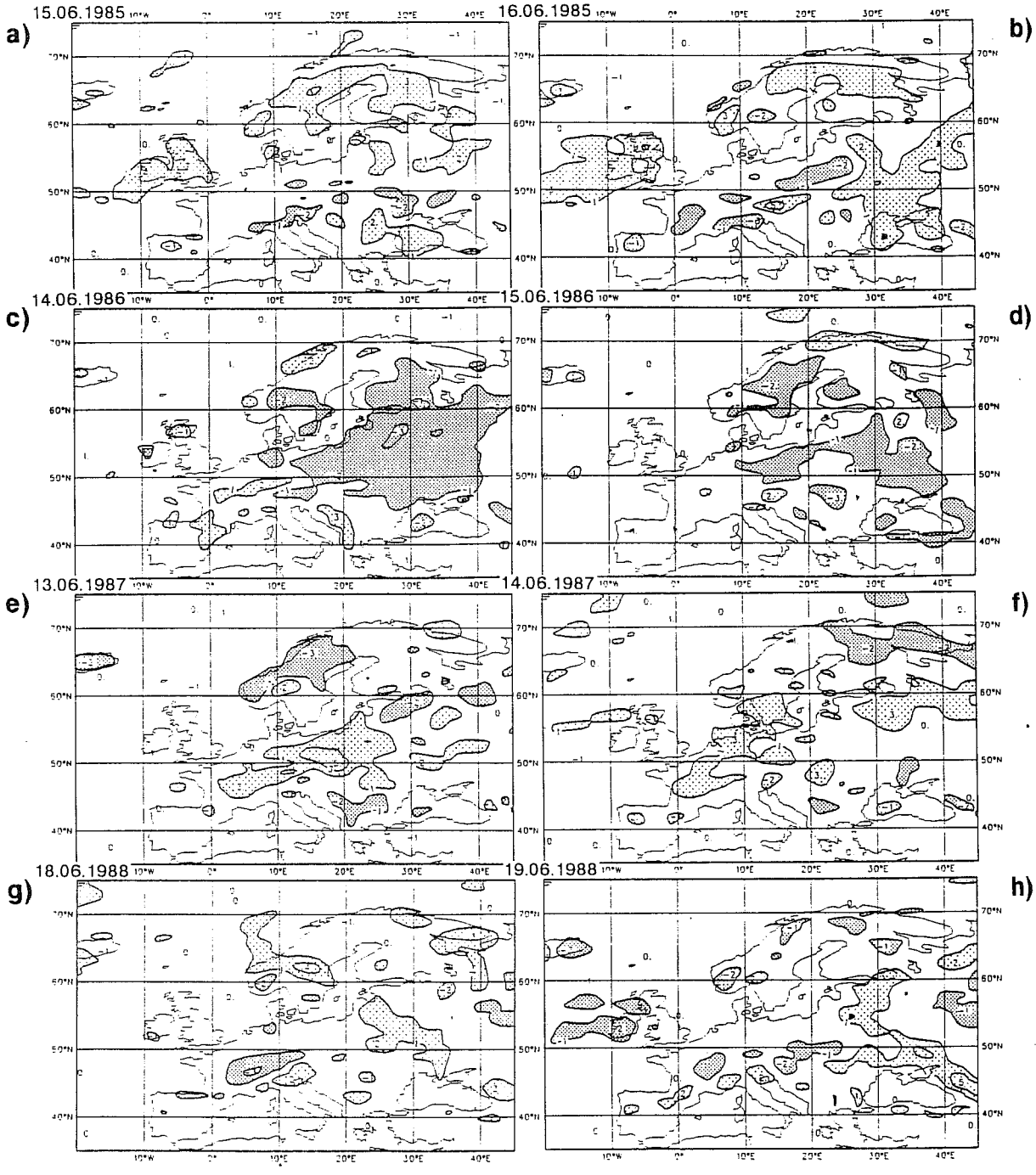

Fig.23 As Fig.20 but for European region.